Master of Science thesis in meteorology

DEVELOPING A PORTABLE METHANE SAMPLING SYSTEM FOR LOW-CONCENTRATION ENVIRONMENTAL APPLICATIONS

Eemi Okko Johannes Seppälä

28.11.2019

Supervisor(s):
Unit Director Markku Oinonen and Assoc. prof. Mari Pihlatie

Examiners:
Prof. Timo Vesala and Assoc. prof. Mari Pihlatie

UNIVERSITY OF HELSINKI
DEPARTMENT OF PHYSICS

PO. BOX 64 (Gustaf Hällströmin katu 2)
00014 University of Helsinki

HELSINGIN YLIOPISTO
HELSINGFORS UNIVERSITET
UNIVERSITY OF HELSINKI

MATEMAATTIS-LUONNONTIETEELLINEN TIEDEKUNTA
MATEMATISK-NATURVETENSKAPLIGA FAKULTETEN
FACULTY OF SCIENCE

Tiedekunta – Fakultet – Faculty	Koulutusohjelma – Utbildningsprogram – Degree programme	
Tekijä – Författare – Author		
Työn nimi – Arbetets titel – Title		
Työn laji – Arbetets art – Level	Aika – Datum – Month and year	Sivumäärä – Sidoantal – Number of pages

Tiivistelmä – Referat – Abstract

Methane(CH_4) is a powerful greenhouse gas and even though the CH_4 concentrations in the atmosphere have been increasing rapidly since the year 1750, there still remains large uncertainties in the individual source terms to the global CH_4 budget. Measuring the isotopic fractions from various CH_4 sources should lead to new knowledge on the processes involving CH_4 formation and emission pathways. Nowadays stable isotope measurements for various CH_4 sources are quite routinely made, but radiocarbon measurements have for long been too expensive and time consuming. For this reason a new CH_4 sampling system for radiocarbon measurements was developed at the Laboratory of Chronology of University of Helsinki. The system allows sampling directly from the atmosphere or from different environmental sources using chambers. To demonstrate the functionality of the system it was tested and optimized in various laboratory experiments and in the field.

The laboratory measurements showed that before combustion of CH_4 to carbon dioxide(CO_2), ambient carbon monoxide(CO) and CO_2 can be removed from the sample gas by a flow for more than 10 hours with a flowrate of 1 l/min. After the CO and CO_2 removal the CH_4 in the sample gas is combusted to CO_2. The combustion efficiency for CH_4 was 100% with a flowrate of 0.5 l/min. After CH_4 is combusted to CO_2 it is then collected to molecular sieves and can be later on analyzed using accelerator mass spectrometer. The laboratory measurements, however, showed that due to adsorption of nitrogen(N_2) to the molecular sieves, the 1g of molecular sieve material used in molecular sample sieve tubes was not sufficient for low concentration samples where the sampling times are very long.

In the field, CH_4 was collected from the atmospheric ambient air at Hyytiälä SMEAR II station, Juupajoki, Finland, and from tree and soil chambers. The radiocarbon content of the atmospheric CH_4 was 102.27 ± 0.02 percent Modern Carbon (pMC) and 101.40 ± 0.02 pMC. These values were much lower than the expected values, indicating a large spatial and temporal variability. The CH^4 collected from chambers closed around tree-stems had a radiocarbon content had of 113.60 ± 0.37 pMC, which was slightly higher than the 108.71 ± 0.37 pMC measured from soil chambers located in the nearby Siikaneva peatland. This indicated that a larger amount of CH_4 emitted from peatland surface was recently fixed near the soil surface and a larger amount of the CH_4 emitted from tree-stem surface was from older origin transported via roots from the deeper depths of the soil. There is, however, a possibility that the lower radiocarbon content from the peatland surface emitted CH_4 was due to a significant contribution from old CH_4 fixed before bomb effect, and which is diffused from deeper depths of the soil. This would explain the results from the autumn campaign where the radiocarbon contents were 91.84 ± 0.03 during nighttime and 104.26 ± 0.03 pMC during daytime. These results also indicated that during the daytime more of the emitted CH_4 is fixed near the surface of the peatland soil. One additional CH_4 sample was collected in January 2019 from the atmospheric ambient air at Kumpula, Helsinki, Finland using a significantly larger molecular sample sieve. This sample had a radiocarbon content of 52.40 ± 0.21 pMC. The old carbon in the sample originated from a fossil methane used in earlier laboratory experiments and indicated that the regeneration process for the larger sample sieve was incomplete.

Overall the system functions very well, while collecting samples from environmental chambers, as the CH_4 concentrations are left to build-up before collecting the sample. For atmospheric samples, for which the sampling times are higher, the sample sieve size and the regeneration time and temperature will have to be further investigated. In the future, more measurements of the radiocarbon content for individual CH_4 sources are needed to provide better knowledge on the CH_4 pathways. This portable system allows an efficient way to collect CH_4 samples for radiocarbon analyzes from various locations.

Avainsanat – Nyckelord – Keywords
Säilytyspaikka – Förvaringställe – Where deposited
Muita tietoja – Övriga uppgifter – Additional information

HELSINGIN YLIOPISTO
HELSINGFORS UNIVERSITET
UNIVERSITY OF HELSINKI

MATEMAATTIS-LUONNONTIETEELLINEN TIEDEKUNTA
MATEMATISK-NATURVETENSKAPLIGA FAKULTETEN
FACULTY OF SCIENCE

Tiedekunta – Fakultet – Faculty	Koulutusohjelma – Utbildningsprogram – Degree programme	
Tekijä – Författare – Author		
Työn nimi – Arbetets titel – Title		
Työn laji – Arbetets art – Level	Aika – Datum – Month and year	Sivumäärä – Sidoantal – Number of pages

Tiivistelmä – Referat – Abstract

Metaani(CH_4) on voimakas kasvihuonekaasu ja sen määrä ilmakehässä on kasvanut huomattavasti viimeisten satojen vuosien aikana. Tästä huolimatta ilmakehän metaanitaseeseen liittyy edelleen suuria epävarmuuksia. Isotooppimittausten avulla on mahdollista kerätä uutta tietoa metaanilähteistä ja niihin liittyvistä prosesseista. Metaanin lähteiden stabiili-isotooppien arvot tunnetaan maailmalla melko hyvin, mutta radiohiilimäärityksien tekemiseen ei tähän asti ole löytynyt edullista ja tehokasta tapaa. Tämän vuoksi kehitimme Helsingin yliopistossa toimivassa ajoituslaboratoriossa uuden näytteenkeräyssysteemin metaanin radiohiilipitoisuuksien mittaamista varten. Systeemin avulla näytteitä pystytään keräämään suoraan ilmakehästä tai ympäristön metaanilähteistä kammiomenetelmin. Osoituksena menetelmän käyttökelpoisuudesta sitä testattiin sekä laboratoriomittauksin-, että kenttäolosuhteissa.

Laboratorio-olosuhteissa tehdyt mittaukset osoittivat, että kontaminaatiota aiheuttavat hiilidioksidi (CO_2) ja hiilimonoksidi (CO) saadaan poistettua näytevirrasta vähintään 10 tunnin keräyksellä, kun virtausnopeus on 1 L/min. Tämän jälkeen metaani poltetaan hiilidioksidiksi. Polttotehokkuus on 100 % uunin ollessa 600 °C ja virtausnopeuden ollessa 0.5 L/min. Hiilidioksidiksi poltettu metaani voidaan tämän jälkeen kerätä näyteseulaan myöhempää analysointia varten. Mitatuista laboratorio- ja kenttänäytteistä huomattiin kuitenkin, että näyteseulojen sisältämää 13X-zeoliitti seula-aineen määrää tulee jatkossa lisätä alkuperäisestä 1 g:n määrästä, jos näytteenkeräys kestää hyvin pitkiä aikoja sillä seula-aine adsorboi myös pieniä määriä typpeä(N_2).

Hyytiälän SMEAR II -aseman läheisyydestä kerätyissä ilmakehän metaani näytteistä havaittiin aikaisempia tutkimuksia pienempiä radiohiilipitoisuuksia 102.27 ± 0.02 prosenttia modernista hiilestä (percent Modern Carbon, pMC) ja 101.40 ± 0.02 pMC, jotka indikoisivat metaanin radiohiilipitoisuuksien vaihtelevan paikallisesti huomattavasti. Hyytiälästä kerätyssä puunrungosta emittoituvan metaanin radiohiilipitoisuudeksi mitattiin 113.60 ± 0.37 pMC. Saman mittauskampanjan aikana Siikanevan suon pinnasta kerätyssä näytteessä radiohiilipitoisuus oli puolestaan 108.71 ± 0.37 pMC. Näiden perusteella puunrungon emittoima metaani olisi vanhempaa kuin suolta vapautuva metaani. Tämä viittaisi samalla siihen, että puun juuret kuljettavat vanhempaa metaania syvemmältä maasta, kun taas metaanin muodostus suolla tapahtuisi lähempänä maanpintaa. Suon emittoiman metaanin matalampi radiohiilipitoisuus voi kuitenkin selittyä myös sillä, että vasta hiljattain muodostuneen metaanin seassa olisi merkittävä osa myös selkeästi vanhempaa, pommipiikkiä edeltävää hiiltä. Tähän viittaisi myöhemmin syksyllä kerätyt näytteet Siikanevan suolta, joissa radiohiilipitoisuudet olivat 91.84 ± 0.03 ja 104.26 ± 0.03 pMC. Lisäksi nämä tulokset viittaisivat siihen, että yön aikana emittoituvassa metaanissa suurempi osa olisi vanhempaa, syvältä maasta diffusoituvaa metaania ja päivänaikana maanpinnan läheisyydessä tapahtuvat prosessit ovat puolestaan voimakkaampia. Hyytiälästä kerättyjen ilmakehän metaani näytteiden lisäksi kerättiin vielä yksi näyte tammikuussa 2019 Helsingistä Kumpulan yliopistorakennuksen katolta suuremman näyteseulan avulla. Kyseisen näytteen radiohiilipitoisuus oli 52.40 ± 0.21 pMC. Näytteen alhainen radiohiilipitoisuus johtui aikaisemmissa laboratoriomittauksissa käytetystä fossiilisesta metaanista ja indikoi näin ollen seulan regenerointiin liittyvistä ongelmista.

Kaiken kaikkiaan näytteenkeräyssysteemi toimii erittäin hyvin, kun näytteitä kerätään kammioiden avulla, jolloin metaanikonsentraatioiden voidaan antaa nousta kammion sisällä ennen näytteiden keräämistä. Ilmakehästä kerättäessä näytteenkeruuaika kuitenkin kasvaa ja tällöin näytteitä täytyy kerätä suurempiin seuloihin, joissa on suurempi määrä seula-ainetta. Näiden seulojen regenerointi prosessin osalta tarvitaan lisää mittauksia, jotta aikaisempien näytteiden kontaminaatiolta vältyttäisiin. Kuitenkin jo nyt keräyssysteemi tarjoaa edullisen ja tehokkaan tavan mitata eri metaanilähteiden radiohiilipitoisuuksia myös vaikeampi pääsyisistä paikoista. Tulevaisuudessa eri lähteiden karakterisointi radiohiilipitoisuuksien pohjalta on hyvä uusi väylä metaanilähteiden tutkimiseen.

Avainsanat – Nyckelord – Keywords
Säilytyspaikka – Förvaringställe – Where deposited
Muita tietoja – Övriga uppgifter – Additional information

Contents

1. Introduction

Limiting the use of fossil fuels is one of the most important means in mitigating the future change in the climate. The ongoing warming is forced by the rising levels of greenhouse gases such as water vapor, carbon dioxide, and methane. Water vapor is the most influent greenhouse gas, but researchers have focused mainly on carbon dioxide and methane due to their much longer atmospheric lifecycles. The atmospheric lifetime for carbon dioxide is approximately 100 years and for water vapor it is closer to 10 days (intergovernmental panel on climate change, IPCC, 2014). Both, carbon dioxide and methane concentrations have been rising rapidly since the beginning of industrial times and therefore it is crucial to achieve understanding of all the mechanisms that has influence on carbon dioxide and methane budgets. Nowadays carbon dioxide sinks and sources are pretty well constructed, but there remains large uncertainties considering the individual methane sink and source quantifications. One of these uncertainties is related to the role of forest ecosystems and trees, which only recently has been suggested as an individual source term for atmospheric methane (Saunois et al., 2016). The various emission pathways for tree emitted methane has further complicated up-scaling the local in-situ measurement to the global scale (Barba et al., 2019). Vascular plants can play a role by transporting methane from soil to the atmosphere and as so act as a conduit from the soil and reverse the attenuating role of soil and or aquatic microbiota (Rusch & Rennenberg, 1998). Keppler et al. (2006) first published a study that showed that methane can be formed aerobically inside the plant tissue. Recently there has been various new studies (Carmichael et al., 2014, Pangala et al., 2017, Wang et al., 2016) implementing that stems of living trees provide an environment suitable for methanogens to colonize the wood of the trees and therefore produce methane which is then emitted to atmosphere through the tree stems. Due to the newly found multiple ways forest ecosystem can emit methane directly to the atmosphere and due to the fact that in many of the global methane budget estimations forest ecosystem have been quantified as methane sinks (because of the uptake by forest soil), it is presumable that carbon cycle models have largely overestimated the amount of which forests ecosystems act as sinks and consume methane.

As the human induced climate change proceeds it is important to understand the exact mechanism how methane is produced and emitted to better acknowledge how climatological changes such as temperature rise or changes in precipitation patterns may infer with methane emission from the source. Better understanding can be achieved by investigating the isotopic composition of methane emitted from the source, because as methane is consumed by methanotrophs or produced by methanogens there is always some fractionation as the lighter isotopes are preferred by microbes (Matson & Harriss, 2009). Different methane sources also vary with different radiocarbon composition as radiocarbon decays during time. Measuring the isotopic fractionation can therefore better the understanding of processes that are dominating in those environmental circumstances. $^{13}C/^{12}C$ measurements are routinely made with mass spectrometers, but for now radiocarbon measurements for methane emitted from low concentration sources such as tree stem surface has been out of reach. This has limited the investigations on methane cycling and carbon cycling as a whole (Pack et al., 2015). A new way to collect samples should bring new insight in to the matter as the $^{14}C/^{13}C$ fractions in many cases offers a significantly better differentiation compared to stable isotope fractions (Palonen et al., 2017). Figure 1, adopted from Oinonen M. et al. 2015. Biofraction measurements of methane for environmental and metrological applications. 22nd International Radiocarbon Conference in Dakar, Senegal, 16–20 November 2015, illustrates the separation power ^{14}C measurements in distinguishing between natural gas and biogas.

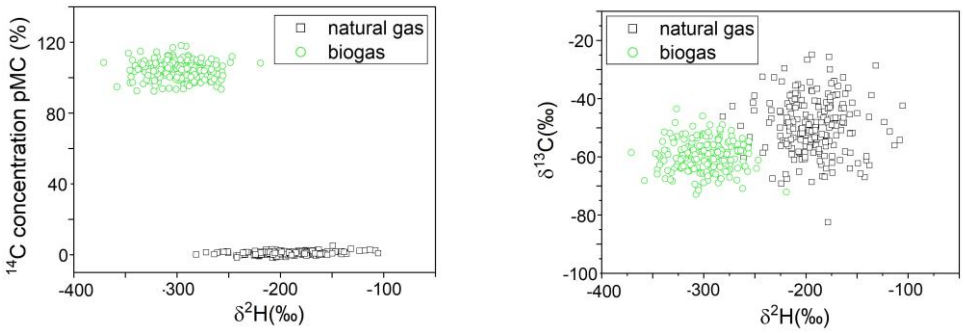

Figure 1: The $^{14}C/\delta^2H$ (left) and $^{13}C/\delta^2H$ (right) differences of natural gas and biogas.

In the Laboratory of Chronology, Finnish Museum of Natural History, in association with the Department of Physics, University of Helsinki, a portable methane sampling

system has been developed and used to analyze bio/ fossil fractions of methane (Palonen et al. 2017). The system has been used to routinely measure bio/ fossil fractions from different high-concentrations methane samples and it has been designed so that measurements from both, atmosphere and environmental chambers should be plausible in the future.

The aim of this thesis is to develop and test the methane sampling system further so that it could be used also for low concentration environmental methane samples, which to this date has been expensive, complex and a time consuming process (or plainly impossible in some cases) (Pack et al., 2015). In this work, the system was tested in laboratory conditions and in the field during the June and September of 2018 measurement campaigns at Hyytiälä SMEAR II station, Juupajoki, Finland to further test the system and to provide rare data on radiocarbon content in different environmental sources. Finally a sample of atmospheric radiomethane from Kumpula, Helsinki, Finland was collected in the beginning of January 2019 to test the sampling method with a larger molecular sample sieve.

This MSc thesis is structured as follows. In the chapter 2, methane as an atmospheric gas is discussed, principles of radiocarbon measurements are given, principle of molecular sieve material is described, a typical carbon dioxide sampling system is presented and, eventually, a path towards methane measurements is provided. In chapter 3, design for the methane sampling system is presented, sample preparation process from methane to pure carbon for Accelerator Mass Spectrometry are described. Furthermore, all the experimental tests made for the system are described. In chapter 4, the results of these measurements are reported including the first radiocarbon measurements from tree stem surface emitted methane. Finally, in chapter 5 the results and future challenges are discussed, including the possible further changes to the system.

2. Theory

In this chapter, methane as an atmospheric gas is discussed in details starting with

methane concentrations in atmosphere and how it has fluctuated in recent history. Then the sources and sinks of atmospheric methane are discussed. In the second part of this chapter, the theory of collecting and measuring radioisotopes fractions from carbon dioxide and methane samples are discussed and previous measurement techniques are presented. Particularly, molecular sieve methodology is discussed in detail as it provides an elegant way to collect carbon dioxide samples. As the properties for molecular sieves used in the carbon dioxide sampling system are considerably well understood (Palonen & Oinonen, 2013), a portable molecular-sieve based carbon dioxide sampling system for radiocarbon measurements has been developed and tested as a collaboration between the Laboratory of Chronology, Finnish Museum of Natural History and Department of Physics, University of Helsinki, (Palonen, 2015). Because studies of ^{14}C of methane from any sources has been limited due to large volume of air that has to be sampled from low concentrations sources, there is a need for a similar system for bioportion measurements for methane.

2.1 Methane in the atmosphere

Methane is the most abundant hydrocarbon in the atmosphere and third most abundant greenhouse gas after water vapor and carbon dioxide. Due to the polar amplification the poleward regions are warming faster than the global average. This may lead to increased methane emissions from thawing permafrost and due to changes in climatological factors such as temperature and precipitations and could therefore enhance the warming of climate as a feedback effect (Etminan et al., 2016). In this chapter we will look at how methane concentrations in the Earth´s atmosphere have fluctuated during historical time span, what kind of role does methane have in the chancing climate, what are the main sources and sinks for atmospheric methane and the isotopic composition for atmospheric methane?

2.1.1 Concentrations in the atmosphere

Like all climatological features, also methane concentrations in the Earth´s atmosphere have fluctuated during Earth´s climatic history. Methane as an atmospheric gas has been studied since the 18th century, first by Alessandro Volta, who described

experiments on flammable gas to father Cambi (Reeburgh W.S 2003) and then by Boussignault (1834, 1864) and Gaultier (1901). They were also the first who tried to estimate the methane concentrations in the atmosphere, but the results were not very reliable with results of first 10 parts per million by volume (ppmv) and later on 0.28 ppmv by Boussignault (1834, 1864) and 95 ppmv by Gaultier (1901). Migeotte (1948) was the first to use infrared absorption measurements in attempt to estimate the methane concentrations in atmosphere, which resulted with a better estimation of 2.0 ppmv, but only after the development of gas chromatography in the beginning of 1950´s has there been possibility for high precision measurements (Bartle & Myers, 2002). This also lead to first continuous time series measurements of methane concentrations in the late 70´s, which suggested that the concentrations of methane in the atmosphere where rising and which was first reported by Graedel and McRae (1980). Even though continuous time series measurements have only been made since then, historical methane concentrations can be studied from trapped air samples in glaciers and in sediments. This has helped scientist to estimate methane concentrations from a much longer time period. In figure 2 the time series measurements from Mauna Loa, Hawaii, is plotted as presented by National Oceanic and Atmospheric Administration (NOAA). The plot shows that methane concentrations have been rising during the last 40 years considerably at the location. Here Mauna Loa was selected as it is surrounded by ocean and therefore resembles a good estimation for global average, but because methane is well mixed in the troposphere, same kind of increasing trend are observed around the Globe. The figure also shows that there has been some variation in the rate of change for methane concentrations. Methane levels where almost stable during the period from 1998 to 2007 and have been rising more rapidly again after the year 2007. This has been mostly explained by the natural variation in sinks and sources of methane and will be further discussed in chapter 2.3.

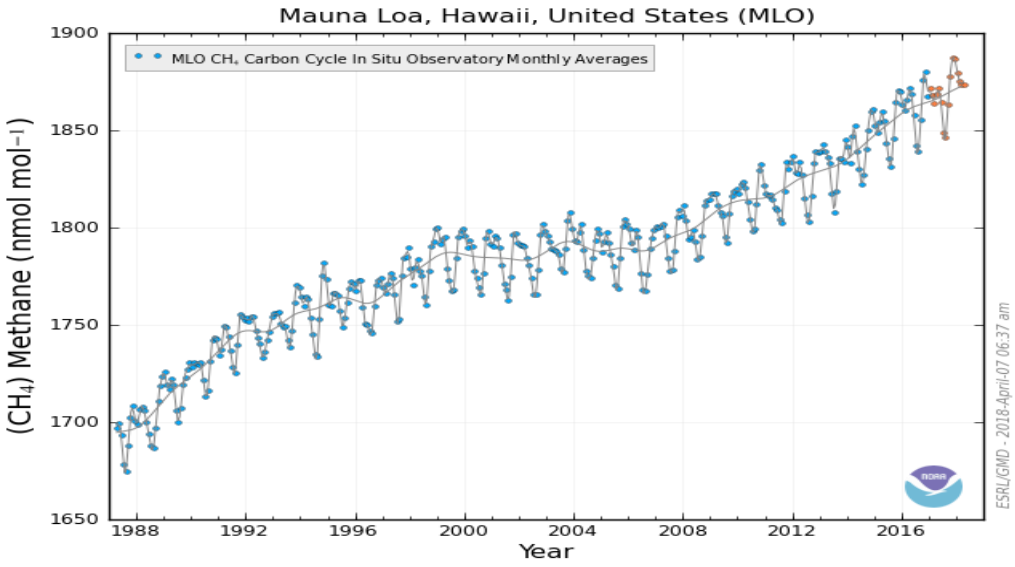

Figure 2: Atmospheric CH_4 concentrations from Mauna Loa, Hawaii, United States from the year 1987 to the year 2018.

Even with the variation in the rate of change in methane concentration, measurements have shown that the concentration have been rising significantly since the beginning of industrial times, after the year 1750. The mixing ratio of methane has almost tripled in the atmosphere from approximately 0.7 ppmv to 1.9 ppmv. From the measurements collected from ice cores in Vladivostok (figure 3) it appears pre-industrial methane concentrations have fluctuated between 0.3 and 0.8 ppmv (Petit et al. 1999). Wuebbles and Hayhoe (2002) reported similar results in the change in methane levels during the span of last 420 000 years and concluded that current methane levels are unprecedentedly high with historical methane concentrations varying between 0.3-0.7 ppmv during the last 420 000 years span. In the IPCC fifth assessment report the record of the methane levels has been expanded to last 800 000 years (IPCC 2014). Even then the historical atmospheric methane concentration has not been higher than the 0.8 ppmv reported by Petit et al. (1999). More recently there has been developed a new continuous flow analyses system by Federer et al. 2009, which allows a high-resolution methane measurement from polar ice. The results of reported minimum and maximum methane concentrations during historical periods do not however differ considerably from the result from previous work done by Petit et al. (1999) and Wuebbles and Hayhoe (2002).

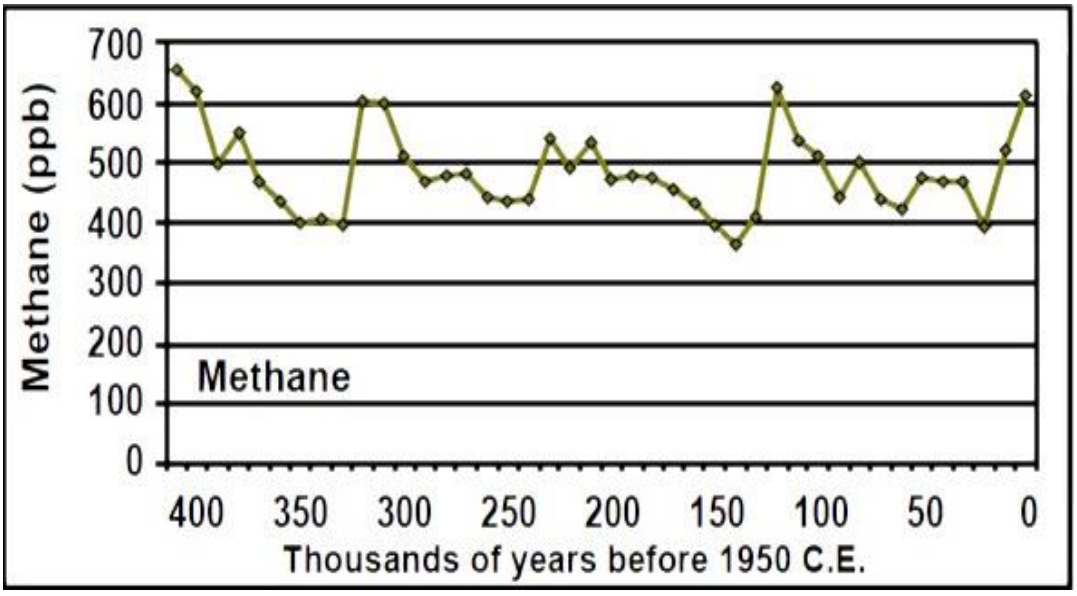

Figure 3: Atmospheric methane concentrations during the last 400, 000 years measured from ice cores from Vostok, Russia (Petit et al. 1999).

2.1.2 Effects on the climate

Earth´s climate is greatly influenced by so-called greenhouse effect. Greenhouse gases act similarly to glass structure in greenhouses, meaning that they are transparent to solar, shortwave, radiation emitted by the sun, but absorb radiation at longer wavelengths which is emitted back to the atmosphere from the surface of the Earth. According to Schwartz (2018); "The greenhouse effect is manifested as the difference between thermal infrared radiation emitted at the Earth surface and that emitted to space at the top of the atmosphere". Because of the natural greenhouse effect, the average surface temperature on Earth is approximately 32 °C greater than what it would otherwise be. It has therefore been a crucial ingredient helping life as we now know it to develop (Schwartz 2018). After the start of industrialization, the amount of greenhouse gases, especially carbon dioxide and methane has increased in the Earth´s atmosphere leading to global warming. Methane is one of the most important greenhouse gases in the atmosphere. Since the beginning of the industrial era, the rising levels of methane concentrations are contributing the second largest additional radiative forcing after carbon dioxide to the total increase in radiative forcing by greenhouse effect (Wuebbles & Hayhoe, 2002)

The radiative forcing, which is measured as W/m² is an imposed change of the planetary energy balance (Hansen et al. 2005). The absorption by methane is strongest at a lower spectrum of infrared region, ~7-13 μm with the most important region being the 7.66 μm band, in which there is only little absorption by water vapor and carbon dioxide (Wuebbles & Hayhoe 2002). The radiative forcing by direct absorption by methane has been analyzed by multiple groups. Myhre et al. (2013) estimated that additional forcing from rising methane levels since 1750 (0.722 ppmv) to 2011 (1.80 ppmv) has been 0.48 W/m². It was slightly less than some previous analyses such as Hansen et al. 2005 and Jain et al. 2000, of which both calculated radiative forcing of 0.55 W/m². Methane however, also absorbs radiation at the shortwave radiation band (near infrared band) which has not been considered in the calculations by Myhre et al. (2013), Hansen et al. (2005) or Jain et al. (2000). This effect was included in the estimation by Etminan et al. (2016), which yielded an added contribution to the radiative forcing estimation from Myhre et al (2013) of nearly 25% and a total direct radiative forcing addition by 0.61 W/m² from pre-industrial times.

In addition to direct forcing by absorption of radiation, methane contributes indirectly to global warming by chemical interactions. In the atmosphere, methane is oxidized in a reaction with hydroxyl (OH) and nitric oxide (NO) and forms ozone, water vapor and as a final product carbon dioxide, all of which are important greenhouse gases as well (Wuebbles & Hayhoe, 2002).

Changes in tropospheric ozone due to increased amount of methane in the atmosphere is the most impactful indirect effect. The total increase of radiative forcing due to increased ozone in the troposphere has been estimated to be between 0.25 W/m² and 0.45 W/m² depending substantially on the location and altitude of the ozone change and with an average value of 0.35 W/m² (Gauss et al., 2006). More recent estimations by Skeie et al. (2011) and Stevenson et al (2013) estimated a total radiative forcing from the year 1750 to 2010 by tropospheric ozone to be 0.44 W/m² (± 30%) and 0.41 W/m² (± 10%), respectively. Model experiments presented by Shindell et al. (2009) showed that almost half of the changes in radiative forcing by tropospheric ozone since the pre-industrial era can be attributed to increases in methane emissions during that

time. The increased amount of methane in the stratosphere will increase stratospheric water vapor, when oxidized. Due to the low amount of water vapor in the stratosphere, and because water vapor is a strong greenhouse gas, this has led to increase in radiative forcing of 0.07 (± 0.05) W/m² between the years 1750 and 2005 (Forster et al., 2007). Increased water vapor due to methane oxidation could also lead to more stratospheric polar clouds, which according to Ramanathan (1988) have ability to enhance the greenhouse effect even further. As a final product methane oxidation produces carbon dioxide, but of which the biogenic portion is already included in the carbon dioxide budget (Wuebbles & Hayhoe, 2002). According to Hansen et al. (2005), the indirect effect of radiative forcing from methane may contribute an additional forcing up to 40% to the direct radiative forcing of methane.

2.1.3 Sinks and sources

After the discovery of rising methane concentrations in the atmosphere in the 70´s and because of the importance of the effects (both direct and indirect) that methane has in the atmosphere, it has become increasingly important to gain a better understanding on all of the processes that impact the amount of methane in the atmosphere. The amount of total annual methane released to the atmosphere, and also the amount removed from it due to different methane sources and sinks, often described as the global methane budget, is quite well constrained annually, but there remains large uncertainties within individual sinks and source terms. These uncertainties play an important role especially for future estimations, where the rate of change in every individual source term has to be factored in (Carmichael et al., 2014). The first estimations to assemble the total global methane budget was made by Ehhalt (1974) and expanded by Ehhalt and Schmidt (1978). Even with the lack of data, this work correctly identified many of the major atmospheric sources and did a very good first estimation of the magnitudes of many of the major source terms in the global methane budget (Reeburgh, W.S, 2003). In their work, Ehhalt & Schmidt (1978) identified paddy fields, freshwater sources, upland fields and forests, tundra, the ocean and enteric fermentation by animals as biogenic sources. They considered radiocarbon free sources as anthropogenic sources so that the first radiocarbon methane measurements (Libby W.F, personal communication with Ehhalt) were used to form an upper limit

for anthropogenic sources. Methane oxidation by OH radicals which by far is the biggest sink for atmospheric methane was identified as well as losses to the stratosphere by eddy diffusion and Hadley circulation. The work, however did not consider oxidation by soils, which has been afterwards estimated to form up to 5% of the total sink (Wuebles & Hayhoe, 2002). The work also recognized the concentration gradient between Northern and Southern hemispheres, which indicated a bigger source term in the Northern hemisphere.

Since the first estimation by Ehhalt (1974) multiple new reviews have been published which have brought new insight to the matter especially on the human induced sources, where for example agricultural and waste related emission have been categorized as anthropogenic sources (Kirschke et al., 2013, Saunois et al 2016). New review from Saunois et al (2016) provides a complete review of all methane sources and sinks based on an ensemble of bottom-up approaches from multiple sources: process-based models, inventories, and data-driven methods, that contributes a source term of ~ 400 Tg/year from anthropogenic sources and ~ 210 Tg/year from natural sources. Even with the new methods used in the review by Saunois et al. (2016), there still remains an uncertainty, especially those related to natural sources from wetlands, which is the greatest natural source for atmospheric methane and can easily accommodate an additional methane source up to 120 Tg/year (~20% of the total budget). Keppler et al. (2006) identified a new source, aerobic methane production from plants, which has a potential to reduce uncertainties regarding methane sources to atmosphere, but which to this date has not been concluded to the global methane budget due to the lack of understanding in this mechanistic pathways in productions of methane (Carmichael et al., 2014).

2.1.4 Emissions from vegetation

Few distinct pathways for the production and emission of methane from vegetation has been identified (Saunois et al., 2016). First, as discussed previously, plants can produce methane in aerobic process induced by UV-radiation. This was first discovered by Keppler et al. (2006), but has been since reported by other studies as well such as Carmichael et al. (2014) and Fraser et al. (2015). Global estimates still

vary by order of 2 (Liu et al., 2015) and therefore more studies are needed so that aerobic methane production by plants can be included in the global methane budget.

Secondly, plants can act as a source for atmospheric methane due a transport mechanism, where methane produced by microbes in anoxic soils, near the plants root zone is transported from the roots to the above ground plant tissue and released to atmosphere through stems and leaf tissue. This is an efficient way to transport methane. The vegetation including trees, draw methane, which has been produced in soils, and releases it directly to the atmosphere without having to go through the aerobic oxidation layer between anoxic soil and atmosphere (Garnet et al., 2005, Rice et al., 2010, Maier et al., 2018). Pangala et al. (2017), estimated that approximately half of all wetland methane emissions in the Amazon floodplain mediated from tree stem surfaces. If this is added to other emission sources from the area, together they would combine up to one-third of the global wetland methane source.

Thirdly, another direct methane emission pathway from vegetation occurs due to the stems of living trees that commonly provide an environment suitable for methanogens to colonize the wood of the trees (Covey et al., 2012). Overall the studies have shown that trees are a significant contributor of atmospheric methane, but the estimates of the total contribution from plants to global methane budget is complicated because of the overlap between methane consumed by upland soils and methane emitted to atmosphere from wetlands. Integrating these plant-mediated emissions to the global methane budget is needed to improve estimates of the future changes in climate, but the mechanisms, spatio-temporal patterns, and magnitudes of these pathways require to be better defined (Saunois et al., 2016).

At present, no studies at the ecosystem or whole plant scale have shown unequivocally that the methane emitted from the plant was actually produced in the plant. The knowledge about the relationship between different mechanisms that stimulate methane production and emission from plants is still lacking (Bruhn et al., 2012). However, a number of studies have measured aerobic methane production at the scale of plant parts and concluded that four stimulating factors have been observed to induce aerobic methane production in plants; cutting injuries and increase in either

temperature, UV-radiation and/ or in the amount of reactive oxygen species (ROS). ROS can react with carbohydrates, nucleic acids, lipids and proteins to give a wide range of products. This production of ROS has been observed to increase with other stresses (increase of temperature or UV-radiation, wounding/ cutting injuries) and may act as a unifying mechanism between stresses that lead to methane production in plants. As discussed previously, plants can take a large amount of water through the roots and transport it via xylem to the leaves, from where it is evaporated and released directly to the atmosphere. The transport of water containing methane through the plant can explain why plants grown in different locations emit methane with different isotopic proportions of carbon, as the water will contain methane from different sources (Nisbet et al., 2009). Soil temperature, pore-water methane concentrations and water table depth best explained the changes in tree-stem emissions between seasons, while wood-specific density and pore-water methane concentrations best accounts for the between-species variations in stem methane emission of trees (Pangala et al., 2015, Terazawa et al., 2015).

2.1.5 Radiocarbon in methane studies

Methane is a compound that consist of one carbon atom and 4 hydrogen atoms (CH_4). Carbon (C) has three different isotopes which exist in the nature. The stable isotopes are in the form of ^{12}C and ^{13}C with ^{13}C being the heavier of the two isotopes. In addition to stable isotopes carbon also exists as a ^{14}C (radiocarbon). It is a cosmogenic radionuclide and heaviest of the carbon isotopes (Lingenfelter, 1963). Radiocarbon, as can be deduced from the name, is radioactive and decays over time (half-life ~5730 years). In the atmosphere, ^{14}C is constantly formed in collisions by cosmic-ray induced neutrons with atmospheric gases at the outer atmosphere in a 14N (n, p) ^{14}C reaction (Matson & Harriss, 2009). After the reaction, the formed ^{14}C is oxidized to carbon monoxide which in turn will be later on oxidized to carbon dioxide and incorporated to global carbon cycle (Pack et al., 2015). Because most of the formations of ^{14}C occurs in the stratosphere, a vertical gradient for ^{14}C in the atmosphere is present. This natural gradient is occurring in the stratosphere and in the tropopause, but is dissipated in the troposphere due to strong mixing at tropospheric altitudes (Manning et al., 1990). An additional portion of carbon has been isolated from the carbon cycle in terrestrial and

marine reservoirs for significantly long periods and therefore, because of the decaying of ^{14}C, has a lower ^{14}C content than the atmospheric carbon dioxide or other recently photosynthetically fixed carbon. In such reservoirs the ^{14}C content can be used to determine the age, when the organism has died. For material that has been isolated for longer than 60 000 years, a term; "fossil carbon" is used as the ^{14}C content approaches 0. The ^{14}C content is often expressed with unit "percent Modern Carbon", pMC, which is frequently used for environmental samples and for post-bomb applications. Unfortunately, there are at least two definitions of pMC. Here, as the Helsinki AMS facility measures $^{14}C/^{13}C$ ratios, -we will use pMC defined by:

$$pMC = \frac{\frac{^{14}C}{^{13}C}_{S[-25]}}{\frac{^{14}C}{^{13}C}_{1950[-25]}} \times 100\% \quad (1)$$

Where $^{14}C/^{13}C_{S[-25]}$ is the measured $^{14}C/^{13}C$ ratio of a sample normalized for isotopic fractionation to a typical wood $\delta^{13}C$ value of -25‰ and $^{14}C/^{13}C_{1950[-25]}$ is the corresponding ratio for a standard sample from year 1950 (Stenström et al., 2011). When the ^{14}C content is over 100 pMC, the carbon is considered modern (Matson & Harriss, 2009). When carbon pools that consist carbon that is considered fossil, or old are released to atmosphere (by for example burning of fossil fuels or coal mining), it decreases the atmospheric $^{14}C/^{13}C$ values and the vertical gradient for $^{14}C/^{13}C$ ratio is enhanced. This also leads to amplification of the greenhouse effect as the carbon dioxide or methane released has not been part of the carbon cycle for millenniums. The $^{14}C/^{13}C$ ratio thus can be used to determine the "fossil fraction" of atmospheric carbon, which measures the amount of carbon released from fossil, ^{14}C free, sources (Manning et. al, 1990).

The natural amount of ^{14}C in atmospheric carbon dioxide was perturbed before the Nuclear Test Ban Treaty in 1963 due to testing of thermonuclear weapons. This effect is often referred as the Bomb effect, and the ^{14}C amount was nearly doubled before the implementation of the treaty. The bomb effect needs to be taken in to account every time a carbon dioxide sample that is considered modern is analyzed (Matson & Harriss, 2009, Levin et al., 2010). Because methane is fixed from carbon dioxide, the methane

sample originating from biogenic or pyrogenic sources also reflects the atmospheric $^{14}C/^{13}C$ ratio of carbon dioxide it was derived from. For this reason, the bomb effect needs to be accounted when analyzing the age of the methane source as well (Lassey et al., 2007).

In addition to decay of ^{14}C, the $^{14}C/^{13}C$ ratio is also affected by isotopic fractionation. In physical, biological or chemical transformations the isotopic composition of a compound depends on involved processes. This is due to different masses between isotopes, which also affects the strength of the chemical bonds formed. Isotopes with different masses react and diffuse at different rates, which leads to changes in isotopic composition in both the initial carbon source and in the final product (Matson & Harriss, 2009). In biogenic processes heavier isotopes are discriminated leading to depletion of ^{13}C and ^{14}C isotopes relative to pyrogenic or fossil methane (Lassey et al., 2007). Studying the isotopic compositions of both methane and carbon dioxide is thus very useful in determining both the global importance of a particular source and the mechanism controlling the production (or consumption) of the source in question (Matson & Harriss, 2009). Usually when determining the ^{14}C isotopic fractionation (including the fractionation due to sampling and graphitization process) using mass accelerator spectrometry, the result are corrected using the $^{13}C/^{12}C$ proportions, which can be measured at the same time and normalized to correspond the age of an average wood (Stenström et al., 2011).

The first radiocarbon measurements for atmospheric methane where conducted by Libby W. F. in the 1950´s and reported by Ehhalt (1974). Since the 1980´s and the advent of accelerator mass spectrometry more measurements have been made by several research groups (Wahlen et al. 1989, Quay et al., 1991, Lowe et al., 1991, Lassey et al., 1993). The measurements have been made in distinct locations mainly at Baring Head, New Zealand or South Pole as a time series (Wahlen et al. 1989, Lowe et al. 1991) and a global distribution of radiocarbon in atmospheric methane was presented by Wahlen et al. 1989 and Quay et al., 1991. A work done by Lassey et al., 2007 summarizes the earlier measurements of radiocarbon in atmospheric methane from 1986 to 2000 (figure 4). The radiocarbon content in atmospheric methane has been rising since between 1986 and 2000 quite linearly from 117 pMC (Percent

Modern Carbon) to almost 130 pMC. In a more recent work Townsend-Small et al., 2012 measured atmospheric radiocarbon contents of more than 135 pMC at the Mount Wilson Observatory, Los Angeles, United States. They hypothesized that the measured methane sample was depleted in radiocarbon compared to a 138.9 pMC background value (extrapolated from Lassey et al. 2007) due to fossil methane sources from the city. The rise of radiocarbon content in atmospheric methane relative to radiocarbon in atmospheric carbon dioxide has mainly been linked to growth in direct release of nucleogenic radiomethane to atmosphere, from water-pressurized nuclear plants. This effect is amplified as atmospheric carbon dioxide that has been consumed after the bomb spike with radiocarbon-enriched carbon is circulated to other carbon pools (Lassey et al., 2007). Since Townsend-Small et al. (2012), there has not been any new published measurement of atmospheric radiocarbon for methane. This further increases the importance for creating new, cheaper and better methods of collecting and measuring atmospheric and environmental methane samples of radiocarbon.

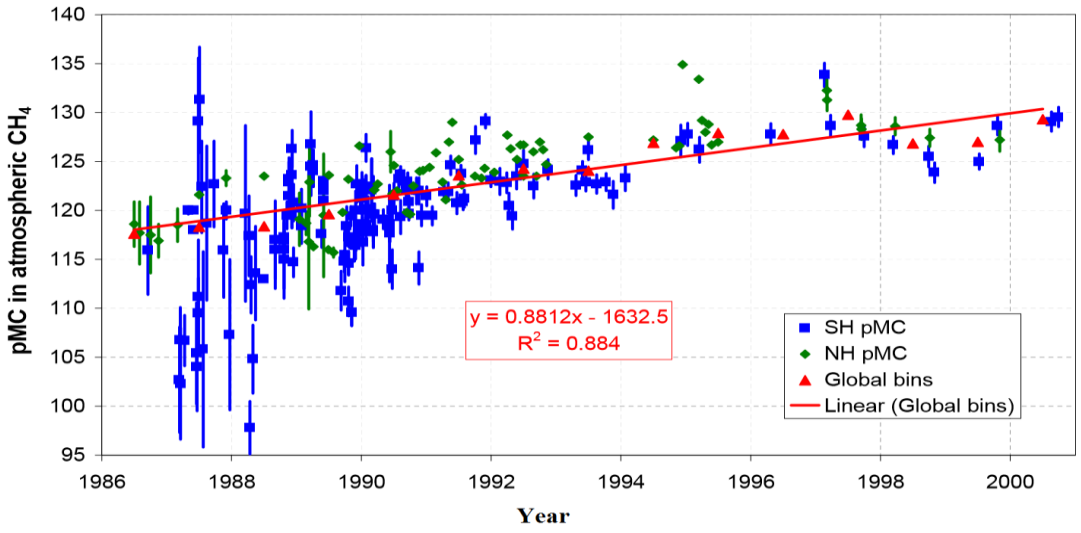

Figure 4: Atmospheric radiocarbon content as pMC for methane as presented by Lassey et al., 2007. Here blue presents measurements made in southern hemisphere and green from Northern hemisphere. Global bins (red) is the global average between hemispheres calculated for each calendar year.

2.2 Adsorption of carbon dioxide using molecular sieves

Before radiocarbon content of a sample can be measured the first step that has to be made is to separate carbon dioxide from the other gases. Few different methods exist for this. Most commonly the separation is done cryogenically by using liquid nitrogen traps, which are also in use in the Laboratory of Chronology (Palonen et al., 2013). Liquid nitrogen reaches temperature of -196 °C in which carbon dioxide is deposited. The problem with liquid nitrogen is that its handling is not practical in field operations (especially in distant locations). There is also a possibility for liquefaction of oxygen that can cause hazardous conditions when oxygen is rapidly evaporated, causing abrupt pressure increases in closed systems. Using liquid nitrogen is also problematic if the samples are collected using chamber methods, as disturbances inside the chamber should be avoided to obtain reliable gas exchange measurements. Using liquid nitrogen and recycling the sample air back to the chamber would cause a significant temperature disturbance as well as a possible pressure drop. Other ways to separate and collect carbon dioxide from sample gas include adsorption to soda lime and/ or molecular sieves (Garnett et al. 2013).

Palonen & Oinonen (2013) investigated the use of molecular sieve materials in AMS measurements for carbon dioxide. Molecular sieve material contains tiny nanometer-scale pores that adsorb molecules. The amount of specific molecules adsorbed is highly dependent on the molecular diameter and the temperature of the sieve material. With suitable selection of pore size and polarity, molecular sieve material can adsorb carbon dioxide highly selectively, enabling sampling from large air volumes in a small amount of adsorbent at atmospheric temperatures (Bayer et al., 1992). The carbon dioxide adsorbed can later on be desorbed and measured by heating the molecular sieve cartridges. The sieves are also non caustic as they can be regenerated without removing the sieve material from the cartridge by connecting the sieve to vacuum line and by heating (Palonen & Oinonen 2013). The most common sieve material used for adsorption of carbon dioxide is the 13X zeolite due to its high selectivity for carbon dioxide (Bayer et al. 1992; Hardie et al. 2005). Palonen & Oinonen (2013) introduced a method for collecting carbon dioxide for radiocarbon analyses, which uses molecular sieve cartridges that contain 1g of X13 zeolite powder that was installed in the middle

of a 300 mm length quartz tube with a quartz filter and quartz wool (figure 5). In their work they tested the carbon dioxide adsorption capacity of the 13X zeolite with ambient air at room temperature (~22 °C) consisting of approximately 400 ppm carbon dioxide and 1000 ppm water vapor. The test showed that, with a flow rate of 0.5 l/min a complete capture of carbon dioxide was obtained during the first 20 min of collection. This means that a saturation point was reached after 10 l of ambient air consisting of 400 ppm of carbon dioxide and 1000 ppm water had passed through the molecular sieve. For precise radiocarbon analyses approximately 0.5 mg of carbon is needed for graphitization (Lassey et al., 2007). The test showed that more than four times of the carbon amount needed for AMS measurements can be collected with molecular sieves with negligible amount of isotopic fractionation. After a breaking point is reached there is a possibility for fractionation due to the fact that zeolites prefer heavier isotopes of carbon dioxide and because water vapor may start to replace captured carbon dioxide (Palonen & Oinonen, 2013).

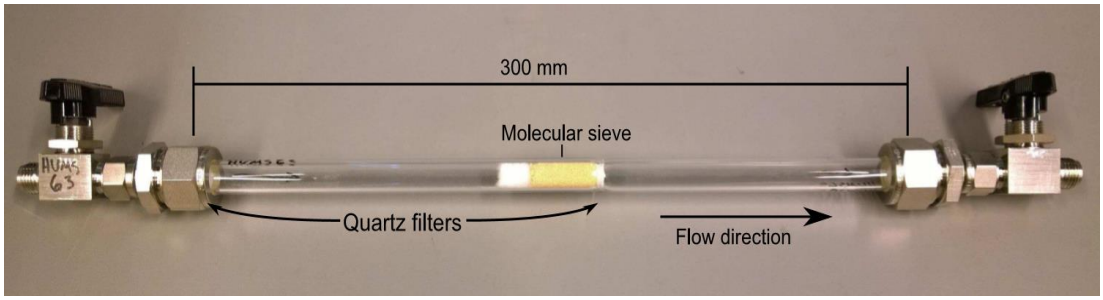

Figure 5: Molecular sieve tube from Palonen (2015).

2.3 Sampling principle for radiocarbon carbon dioxide samples

Palonen (2015) introduced a portable system for collecting samples from atmospheric carbon dioxide. Because the methane sampling system has been designed on the basis of the carbon dioxide sampling system it is beneficial to first subscribe the basic principles of how the carbon dioxide sampling system works. A schematic figure of carbon dioxide sampling system for radiocarbon measurements is presented in figure 6. First the sample air is cycled through the Nafion-dryer (PD-100T-12-MKA, Perma Pure), which has the capability to remove most of the water from the sample gas that

is collected. According to Palonen (2015), after the Nafion dryer, less than 1 parts per thousand (ppt) of water remains in the gas flow with a flow velocity of 1 l /min. The system uses the Nafion dryer in a recirculation mode so that the sample gas is circulated first through the inside of the Nafion tubes and then, as the gas is flowing out of the system it goes through the outside of the tubes that are in lower pressure. Water will then penetrate the tube wall to the low-pressure-side and will not be captured by the sieve grains and will then be returned to the target gas chamber. This minimizes the drying of the target chamber air and maximizes the carbon dioxide trapping efficiency of the sieve grains. The lower pressure is due to the pressure-step at the flow controller. A LI-840A analyzer (LI-COR inc.) is used to measure the carbon dioxide concentration in the flow and to check that the water removal is efficient.

Chamber measurements are commonly used for sample collection and flux measurements by isolating a specific volume of target gas from ambient air using a chamber, which is installed on top of the environmental source. For chamber measurements of ^{14}C, before collecting a sample from a target gas chamber, the chamber must be purified from atmospheric carbon dioxide. This can be done by using larger molecular sieves scrubs which consist of 20g of the same 13X-zeolite adsorbents that is used in the previously described sample sieve tubes and circulating the air from the closed chamber until ambient carbon dioxide has been successfully removed. The scrub is isolated or included in the gas flow with a 4-way valve. Carbon dioxide measurement with the Li-840A analyzer can be used to check that the carbon dioxide removal has been efficient, before starting the sample collection to the molecular sieve. One scrub can adsorb up to 500 l of atmospheric air that has been taken through the Nafion dryer (> 1ppm H_2O). The flux of carbon dioxide from the source (e.g. soil) to the target chamber can be measured as the concentrations inside the chamber are building up. The flux of carbon dioxide is then calculated from the slope of increased concentration inside the chamber over the chamber closure (Pumpanen et al., 2004). Carbon dioxide concentration measurement can also be used to determine the duration for the sampling so that a sufficient size sample for AMS measurements is collected. Graphical user interface and data logging of the Li-840A are handled with a rugged tablet PC (Xplore Bobcat, IP 65), which is also used for note-taking during the sampling. After the Li-840A analyzer, the sample air is taken through the sieve

cartridge which adsorbs all of the carbon dioxide and water from the sample flow. After carbon dioxide has been captured to the molecular sieve, water will be recirculated back to the outflow of the system and remaining gas will be returned back to the target chamber which will significantly reduce the pressure drop inside the chamber (Palonen, 2015). The system also allows sampling directly from the atmospheric air and has been tested for both, atmospheric and soil air measurements (Palonen et al., 2018). After sufficient sized sample has been collected, gas flow can be circulated pass the molecular sieve by closing the valves in the molecular sieve cartridge and opening the bypass valve. The system has been designed so that three carbon dioxide samples for radiocarbon measurements can be collected at one sampling session (Palonen 2015).

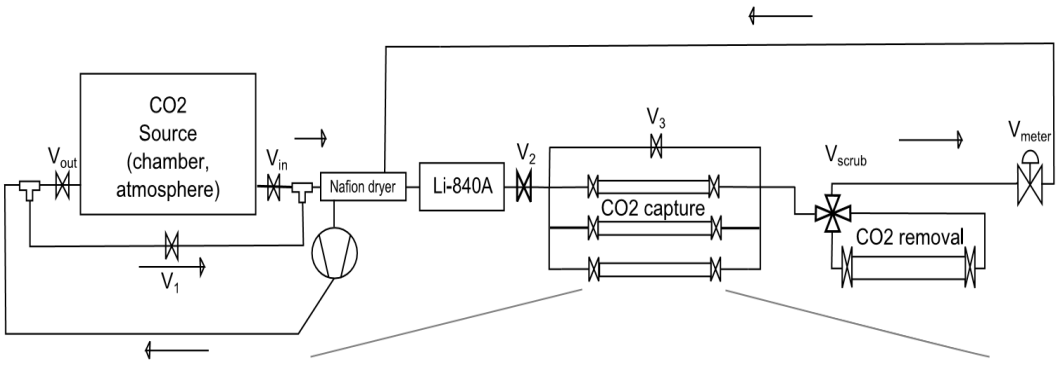

Figure 6: Schematic picture of the portable carbon dioxide samplin system as presented in Palonen (2015).

2.4 Towards a methane sampling system for radiocarbon

Currently there is no published results for ^{14}C signal of methane emitted from tree canopy or tree stems, which both have been reported to emit methane, possibly contributing a significant amount to global methane budget (Machacova et al., 2016, Pangala et al., 2017, Wang et al., 2016). Measurements of local atmospheric ^{14}C methane have been made by numerous groups on locations such as Baring Head, New Zealand and Los Angeles, United States (Lassey et al., 2007, Lowe et al., 1991, Wahlen et al., 1989, Townsend-Small et al. 2012, Quay et al., 1999). The method used for atmospheric methane radiocarbon measurements have been reported by respective groups and have required air samples of volumes from 100 liters (Townsend-Small et

al., 2012) to 20 000 liters (Wahlen et al., 1989). Because of the large volume of air that has to be collected, these techniques are not suitable for chamber measurements. Garnett et al. (2012) and Leith et al. (2014) reported a different technique for measuring radiocarbon from methane emitted from the surface of peatlands. This method is suitable also for other high concentration sources such as wasteland and rice paddies, but it is not suitable for atmospheric measurements because for a sufficient amount of methane collected to a 30 liters bag, a concentration of approximately 30 ppm has to be reached. Another problem with the technique subscribed by Garnett et al. (2012) is that the system does not remove atmospheric air as the concentrations are building up and when the sample is collected ambient air is allowed to enter the chamber to avoid a vacuum inside the chamber.

As discussed, few methods exists that are used to measure radiocarbon content from low methane concentration in environmental sources and from the atmosphere. In principle the sampling processes for AMS measurements are thought similar. First the air is collected and purified from other carbonaceous gases (carbon dioxide, carbon monoxide) and water vapor. Carbon monoxide can be removed from the gas stream by either combusting it to carbon dioxide in a temperature where methane is not yet combusted (typically 290 C°) or by using Schutze reagent, Soffnocat 423 (or Moleculite ®) that oxidizes carbon monoxide to carbon dioxide. Carbon dioxide can be removed by either using molecular sieves, soda lime or liquid nitrogen traps, as discussed earlier. Molecular sieves and liquid nitrogen traps can also be used to remove water vapor from the gas stream. After the contaminating gases have been removed, methane is combusted to carbon dioxide and trapped again using either molecular sieves or liquid nitrogen.

Although a major simplification to the actual reaction mechanism that involves many free radical chain reactions, the catalytic combustion reaction for methane can be represented as following (Lee et al., 1995):

$$CH_4 + 2\ O_2 \rightarrow CO_2 + 2\ H_2O \qquad [2]$$

From the equation [2], it is possible to see that for every methane molecule, two water

molecules are formed. The more abundant and stronger binding water molecules have a tendency to replace carbon dioxide in the molecular sieves (Palonen & Oinonen, 2013). Therefore, for efficient trapping of carbon dioxide, it is important to prevent water reaching the molecular sieve material.

Typical radiocarbon measurement requires 1 mg of carbon at the AMS facility (Palonen, 2015). The sampling time to obtain such an amount is dependent on the used flow rate and on the methane flux to the chamber from the emitting surface area (or from the atmospheric methane concentrations, when collecting the sample directly from air). The concentration level inside the chamber decreases as the sample is collected to the sieves depending on the size of the chamber and on the methane flux to the chamber. For purposes to collect a sufficient amount of methane for AMS analyzes, the time needed to collect the sample can be estimated as a function of flow rate and average methane concentration in the target chamber (or atmosphere) using the ideal gas law first represented by Clapeyron (1834):

$$pV = n\mathrm{RT} \qquad [3]$$

from which the amount of gas in moles is:

$$\mathrm{n} = \mathrm{pV} / \mathrm{RT} \qquad [4]$$

Here n represents the amount of sample gas in moles, p is the pressure inside the sampling system (atmospheric pressure in fields measurements), V is the volume of air that flow through the molecular sieve, which depend on the time sample is collected and on used flow rate so that $V = tu$, in which t is the sampling time and u is the flow rate used. R is the universal gas constant (8.314 J / kg K) and T is the temperature inside the target chamber (air temperature). Now, T and P can be assumed to remain constant during the sampling as the one of the advantages of using the portable methane sampling system is that there is no significant pressure drops or temperature disturbances inside the chambers when the recirculation mode is used. From here the moles amount can be converted to mass (gram) simply by multiplying n by individual molar mass. In field measurements $u \sim 0.001$ m³ /min and methane concentrations are

presented usually as ppm (10^{-6}). The total amount of carbon in a methane sample, can be then determined from:

$$M = m\ C\ (Ptu\ /\ RT) \quad [5]$$

Molar mass of carbon, m is 12.01 g/mole, and C is the average methane concentration.

Methane that has been converted to carbon dioxide can then be measured by accelerator mass spectrometry using standard graphitization methods.

3. Methods and measurements

In this chapter, a portable field-compatible methane sampling system is introduced for ^{14}C measurements. Then AMS ^{14}C measurements are described, examples being bio/fossil fraction measurements for biogas/natural gas mixtures (Palonen et al., 2017). To evolve towards field measurements, a series of laboratory measurements were performed with the portable methane sampling system to determine the functionality of the system in low concentration field conditions. First the functionality of individual components and their efficiency was measured in laboratory. Afterwards the system was used to collect methane samples first from laboratory conditions with different methane concentrations to demonstrate the functionality for low concentration measurements and then from field at different environmental methane sources using chamber methods and from atmosphere. The method used to determine both individual efficiency of components and the system as a whole are presented in this chapter.

3.1 Portable methane sampling system

In figure 7, the schematics picture of portable methane sampling system is presented. First the sample is taken through a Nafion dryer, which as in portable carbon dioxide sampling system is used in recirculation mode and removes most of the water in the gas stream. After this carbon monoxide is removed using a Moleculite catalyst (Molecular Products Limited, Moleculite ® 8-14 mesh) that converts carbon monoxide

to carbon dioxide through an oxidation process. After Moleculite catalyst sample gas goes through two similar larger molecular sieve scrubs than the ones described with the carbon dioxide sampling system, containing roughly 20g of 13X zeolite molecular sieve material in each scrub, which remove all of the carbon dioxide (including oxidized carbon monoxide) and the remaining water from the gas flow.

After impurities have been removed, methane is combusted at 600 °C to carbon dioxide in a combustion oven that consists of a tubular miniature oven of size 70 mm x 70 mm x 70 mm and a 20 mg catalyst (that has been fixed inside the quartz tube with quartz wool). Both, combustion unit and carbon monoxide/ carbon dioxide removal can be bypassed with a 4-wave valve. Palladium- and platinum-based catalysts are considered to be excellent for low-temperature combustion of methane. Usually Palladium-based catalysts are more suitable for oxygen rich conditions and Pt-based catalysts function better in fuel rich conditions (Burch & Loader, 1994). To find the most efficient catalyst for purposes of both low and high concentrations sources of methane, preliminary tests were performed by Palonen et al., 2017. They used commercial Pd/Al2O3 (Alfa Aesar, Product No. 11 711 and 89 114) and Pt/Al2O3 (Alfa Aesar, Product No. 11 797 and 89 106) catalysts both in powder- and pellet-forms. The tests were done with 0.5%-CH_4 20%-O_2 synthetic air. Based on the initial tests, Pd/Al2O3 in powder-form proved to be the most suitable. However, the catalyst performance might be influenced by other conditions, such as the methane concentration and pressure during the combustion process (Palonen et al., 2017).

The sample gas goes through a Li-840A analyzer, which can be used to measure the carbon dioxide in the sample gas if the carbon monoxide/ carbon dioxide removal is bypassed. When both, carbon dioxide and carbon monoxide are removed, the Li-840A analyzer can be used to measure the methane concentration in the gas flow after methane is combusted to carbon dioxide. After Li-840A the carbon dioxide converted methane can be collected to smaller molecular sieves which again are similar to ones used with carbon dioxide sampling system consisting of 1g of 13X zeolite molecular sieve material. Flow rate during the sampling can be controlled by a flow controller (Swagelok VAF-G2-07L) that has been installed to the system after the smaller molecular sieves. Now that methane has been sampled and collected, water can be

recirculated back to the gas flow and returned to the target (chamber/ atmosphere). Due to this there will not be a significant pressure drop inside the target and sampling can be continued until there is sufficient amount of sample, or as long as the molecular sieves scrubs for carbon dioxide removal are saturated. This, in theory, allows both sampling from atmospheric air and sampling from target chambers. Li-840A is connected to rugged tablet personal computer (Xplore Bobcat, IP 65), which is used for graphical user interface, data logging and note-taking during sampling. The system is easily transportable as it can be powered using either rechargeable battery or if available directly from external power source (Palonen et al. 2017).

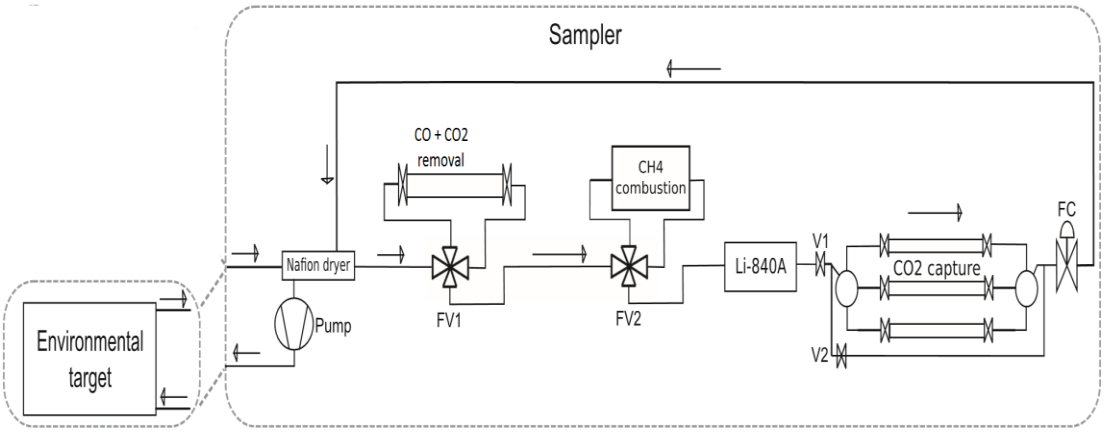

Figure 7: Schematic picture of portable methane sampling system. Figure from Palonen et al., 2017.

3.2 Sample graphitization and AMS radiocarbon measurements

After the carbon dioxide sample has been collected to the molecular sieve it can be desorbed from the sieve by using the HASE preparation line (Palonen et al., 2013) that has been developed by the Department of Physics, UH, and installed at the Laboratory of Chronology. A schematic figure of HASE line is presented in figure 8. The molecular sieve tube is connected to HASE line and covered with an oven. The carbon dioxide sample is released from the sieve first by pumping the HASE line to vacuum and then heating the molecular sieve in an oven. First the sieve is heated for 30 minutes in a temperature of 250 °C in which most of the water vapor is desorbed and hydrothermal damage can be avoided (Palonen, 2015). Then the sieve is heated 2 hours

at 550 °C so that most of the carbon dioxide is desorbed. A cryogenic trap (liquid nitrogen) is installed in to the HASE line which traps all of the water vapor and carbon dioxide. After the sample is collected from the sieve, the cryogenic trap is isolated from the rest of the HASE line with plug valves and water vapor is separated with an ethanol trap (-70 °C). After water is separated, carbon dioxide sample can be collected cryogenically to a storage vial and the amount of carbon can be measured using the calibrated volume and a MKS 925C Micropirani Vacuum Transducer pressure sensor (Palonen, 2013).

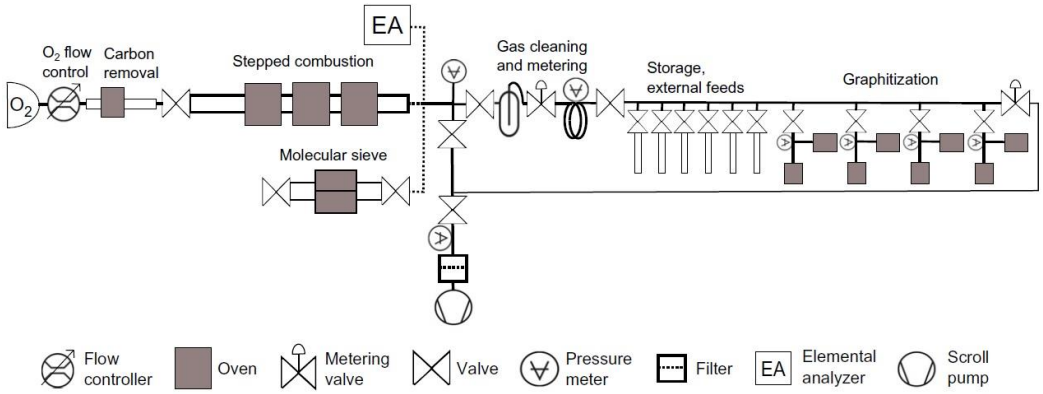

Figure 8: A schematic picture of the HASE-preparation line from Palonen et al. 2013.

The HASE line contains four automated graphitization reactors separated by plug valves. After carbon dioxide sample has been desorbed, collected with cryogenic trap in the sampling line and separated from water vapor, the size of the sample is then measured and can be afterwards graphitized with one of the graphitization modules consisting of two separate ovens. The graphitization method follows the method described originally by Slota et al., 1987 where, carbon dioxide is reduced to carbon monoxide in a reaction with zinc and the carbon monoxide then disproportionate to graphite over iron. Both of the ovens can be placed over a 50-mm-long, 6 mm-outer diameter quart tubes with a volume of 2.0 ml, with one of the tubes filled with approximately 300 mg (250-350 mg) of zinc and the other containing about 3 mg (2.5-3.5 mg) of iron. After the carbon dioxide sample is moved to graphitization reactor, the automated graphitization program first heats the zinc oven to 450 °C and after one hour the iron reactor is turned on and heated to 650 °C. The total graphitization process takes about 4h and the final product can be then pressed and analyzed with AMS

(Palonen et al., 2013). Without going to further details, a simplified description of AMS is following, Cesium-ion beams are targeted to the graphite targets which cause carbon atoms to be released. The released carbon atoms are then accelerated towards the magnetic field. Inside the magnetic field, because of the mass difference between different carbon isotopes, heavier isotopes of carbon will have a different trajectory to the lighter isotopes and because of the high energies of individual atoms, they can be detected and measured (Matson & Harriss, 2009, Tikkanen et al., 2004).

To demonstrate the accuracy for methane bioportion measurements using the portable methane sampling system, the system has been tested with known different mixtures of bio and fossil methane gases provided by Gasum OY. The natural gas, assumed 100% fossil was imported to Finland along a pipeline from Western-Siperia, Russia and collected from Gasum natural gas facility at Imatra. Biogas was collected from Gasum biogas facility at Kujala, Lahti. The two gases were mixed with automatic mass flow controllers (Vögtlin GSCA9TA-FF21), with accuracy of 0.2% (provided by manufacturer) to produce reference samples with 100%, 50%, 30%, 10%, and 0% (fossil gas) biogenic methane, sampled with the system described previously and measured with AMS. The results showed that the measured bioportion fractions were well within the existing standardization (3%) with the average difference between measured and mixed biofractions of 0.1% and maximum difference of 0.6% (Palonen et al., 2017).

3.3 Laboratory measurements

To determine the suitability for radiocarbon analyzes for environmental methane, the portable methane sampling system has been tested in further laboratory measurements and in field. First, methods for measuring the functionality of the new inserted Moleculite ® catalyst, which is installed in front of the molecular sieve scrubs are presented. Next the methods to further analyze the carbon dioxide adsorption of 13X zeolite molecular sieves and combustion of methane are presented. Finally the methods used to perform measurement series for different methane concentrations are described.

3.3.1 Carbon monoxide removal

Before methane can be combusted to carbon dioxide, it is critical that all other carbonaceous gases will be removed from the flow. Basically this means carbon monoxide and carbon dioxide have to be removed. If not removed from the sample gas, carbon monoxide is combusted to carbon dioxide during methane combustion and could therefore lead to overestimations of ^{14}C in methane. Usually, the amount of carbon monoxide in the atmosphere is 20 times smaller (there is large temporal and spatial variation in the atmospheric carbon monoxide concentrations compared to carbon dioxide or methane) than the amount of methane and the radiocarbon content is not expected to alternate largely between the two gases (Palonen et al., 2017). However, for some cases the carbon monoxide concentrations can be substantially higher than the present average atmospheric amount (Petrenko et al., 2008). To eliminate the uncertainty related to contamination due to carbon monoxide, a Moleculite ® (Molecular Products Limited, Moleculite ® 8-14 mesh) catalyst has been installed to the portable methane sampling system. Moleculite ® oxidizes carbon monoxide to carbon dioxide, which can then be removed from the sample gas flow together with other carbon dioxide content in the gas.

To test the functionality of the Moleculite® catalyst, a synthetic air/ carbon monoxide mixture gas (borrowed from INAR (Institute for Atmospheric and Earth System Research) with 20 ppm carbon monoxide was installed to the inlet tube of the portable methane sampling system. Carbon monoxide content in the outlet tube was measured with EL-USB-CO carbon monoxide datalogger (Lascar electronics, UK). The combustion oven was bypassed with a 4-way valve and another 4-way valve was used to direct the gas flow through the Moleculite® catalyst or bypass the catalyst during the measurements. To measure if flow rate has an effect on the oxidation process the flow rate was increased during the test step-by-step from 0.5 liters per minutes to 2.0 liters per minutes.

3.3.2 Carbon dioxide removal

When collecting methane samples for radiocarbon analyzes from different

environmental sources, a complete removal of contaminating carbon dioxide from both ambient atmospheric air and from the source (soil surface flux etc.) is necessary as there is roughly 200-times more carbon dioxide in the atmosphere compared to methane. As discussed previously, methane requires to be converted to carbon dioxide before graphitization and eventual measurements with AMS. In the portable methane sampling system the removal of carbon dioxide is done with two scrubs with 20 grams of 13x zeolite adsorbent which is commercially available in both powder (45-60 nm mesh-size) and pellet form (0.5 mm mesh size).

The adsorption process using molecular sieves is temperature dependent and some of the carbon dioxide is already desorbed at room temperatures (Palonen & Oinonen, 2013). When the methane sample is combusted at the combustion oven, the sample gas is heated, which may affect the adsorption capacity of the molecular sieves. Measurements for carbon dioxide removal were conducted by circulating atmospheric air at room temperature consisting of 400 ppm carbon dioxide and 1000 ppm water with a flow of 1.0 liters per minute through and monitoring the carbon dioxide concentrations in the flow after the scrubs with Li-840A analyzer. After the Li-840A analyzer a carbon dioxide sample was collected to a smaller molecular sieve (containing 1 g of 13x powder). The monitored carbon dioxide concentration were then analyzed to see when the scrubs were saturated and the carbon dioxide removal efficiency started to decrease. The carbon dioxide sample that was collected to smaller molecular sieve was measured later on in the HASE preparation line illustrating if a small amount of carbon dioxide below the detection level of Li-840A analyzer was not captured by the scrubs. The sample was collected to a molecular sample sieve during the first three hours of measurements after which the molecular sieve was closed and flow was directed past the sieve.

Water adsorption decreases the capacity of the sieve material to trap carbon dioxide. To see if the adsorption capability could be enhanced by either inserting another water removal trap using magnesium perchlorate or a cooling mechanism using an ethanol trap that has been cooled to 70 °C before the molecular sieve were also tested with a combustion oven set to temperature of 600 °C.

3.3.3 Combustion of methane

Preliminary test were conducted for different commercially available palladium and platinum catalyst by Palonen et al. (2017), with palladium-aluminum powder (Pd/Al2O3 (Alfa Aesar, Product No. 11 711 and 89 114) proving to be the most suitable when there is a need for sampling of both high and low concentration methane samples. Palladium catalyst usually function well with high oxygen mixtures such as those from environmental sources. The combustion efficiency is highly dependent on the flow rate of the sample gas (Palonen et al., 2017). Complete combustion of methane occurred already at ~400 °C with a flow rate of 0.1 liters per minutes, but with a flow rate of 1.0 liters per minutes the combustion was not complete even at the temperature of 600 °C. In earlier unpublished test it has been observed that if temperatures are increased clearly over the 600 °C limit, a rapid decline in combustion efficiency with palladium-aluminum powder catalyst occurs due to the damage directed to the catalyst. For this reason the combustion is usually done with a flow rate less than 1.0 liters per minutes at temperature of 600 °C.

In this work, additional tests were made to measure if the combustion process depend on the pressure inside the system when the methane is combusted, or if methane concentrations of the sample gas affects the combustion. To test these, a synthetic air (21% oxygen, 79% nitrogen) was connected to the system with a flow controller (Vögtlin GSC-B4TA-FF23) and a natural gas bottle consisting over 96% methane was connected to another flow controller (Vögtlin GSCA9TA-FF21). This allowed mixing of these two gases to create different methane concentrations which could then be combusted in the combustion unit. This also allowed, with constant amount of gas flowing in to the system, the adjustment of pressure with another flow controller (Swagelok VAF-G2-07L). During the measurement, combustion efficiency could be monitored with the Li-840A analyzer from the amount of carbon dioxide after the combustion unit. Li-840A could also be used to measure the pressure inside the system.

3.3.4 Radiocarbon measurement for methane as a function of concentration

Before taking the methane sampling system to field, it was first tested with different

concentrations of fossil methane to measure the background radiocarbon content for the system and verify how the system works with low concentration methane samples. Tests were done using a gas mixtures of a synthetic air that consist of 79% nitrogen(N) and 21% oxygen (O_2) and another gas mixture consisting of 1000 ppm fossil methane and synthetic air. Both gases were provided by AGA and connected to the system. The gases were mixed using two flow controllers (Vögtlin GSCA9TA-FF21 for 1000 ppm methane gas and Vögtlin GSC-B4TA-FF23 for synthetic air) to achieve different methane concentrations from 100 ppm to 2 ppm in the sample gas flow. After mixing the gases, the samples were then combusted to carbon dioxide and trapped with molecular sieves using the portable methane sampling system at a flow rate of 0.5 l/min.

The concentration measurement series was eventually done with two different kind of setup. The first series was done in June 2018. Five samples for radiocarbon analyzes of fossil methane were done using different (100 ppm, 25 ppm, 10 ppm, 5 ppm and 2 ppm of methane) concentrations and the samples were collected using the smaller molecular sieve cartridges with 1 g of molecular sieve material. In the graphitization process, as the carbon dioxide combusted methane was released from the sieves first only ~ 0.5 mg of carbon could be released with the sample of 100 ppm methane. With the sample from 25 ppm methane concentration, only ~ 0.15 mg of carbon was released. With concentrations of 10 ppm or less methane the amount of released carbon from the sieves became even less and therefore graphitization was not feasible. After graphitization the samples from 100 ppm and 25 ppm methane were measured with AMS and from the results the $^{14}C/^{13}C$ fractions and the age of the carbon could be determined. As the sieves had been tested earlier to be capable of adsorbing sufficient amount of both carbon dioxide and water (see chapter 2.1), it was likely that the problem was related to molecular sieve material being able also to adsorb slight amounts of nitrogen (Deng et al., 2012). For this reason, in the second measurement series to avoid saturation by nitrogen, the samples were collected to bigger molecular sieves consisting approximately 30 g of molecular sieve material. adsorbed nitrogen does not have an effect later on as it is removed during the graphitization process. A total of four samples were made using 75 ppm, 25 ppm, 8 ppm and 2 ppm methane concentrations of fossil methane. After the samples were sampled and collected they

were then desorbed and graphitized in the HASE-preparation line and the ^{14}C contents were measured with AMS. The result should show if measurement in atmospheric conditions and especially measurements from tree emitted methane with even lower concentrations are plausible using the portable methane sampling system.

3.4 Field measurements

The first samples using the portable methane sampling system were collected from Hyytiälä SMEAR II measurement station, Juupajoki, Finland, Siikaneva peatland nearby Hyytiälä, and from the rooftop of the department of Physics, University of Helsinki in Kumpula, Helsinki. A total of 7 methane samples were collected. In figure 9 the sampling system, and both, tree-stem chamber and soil chamber are presented. Three samples from atmospheric methane (two from Hyytiälä and one from Kumpula), three soil surface emitted methane samples from Siikaneva peatland and one sample from tree-stem surface emitted methane of silver birch (*Betula pendula*), located at moist soil, Hyytiälä were collected.

Figure 9: Pictures of Portable methane sampling system (left), soil chamber (middle) and tree stem chamber (right) taken from the field from Siikaneva and Hyytiälä stations.

Soil emitted ^{14}C methane samples were collected from Siikaneva mire (Siikaneva 1), located approximately 10 km southwest from the Hyytiälä SMEAR II station. First sample was collected during the June campaign and two more in September. Samples

were collected from a soil chamber, volume of 0.030 m^3, which was inlayed to the surface for approximately 5 cm depth below the moist soil surface, so that the chamber was isolated from ambient air by water content around the chamber. Additionally a fan was installed inside the chamber to enhance the mixing of air. Contamination from atmospheric methane and from disturbances due to closing the chamber were reduced using the sampling system at recirculation mode for one hour with flow rate of 1 liters per minutes. The methane concentrations inside the chamber during the flushing was monitored by removing carbon dioxide from the flow with X13 zeolite scrubs and then combusting the methane to carbon dioxide and by measuring the carbon dioxide concentration in the flow with the Li-840A analyzer. After one hour of flushing, most of the contaminating methane in the chamber was combusted to carbon dioxide. When the flushing had been carried out, the chamber was left undisturbed so that the methane concentrations inside the chambers would build up. After three ours, the concentrations inside the chamber had increased to ~30 ppm/methane, sufficient for sample collection, and the samples were collected to molecular sieves. The sampling was carried out over a duration of one hour, for which a sample of ~0.5 mg of carbon should have been achieved according to the calculations (average methane concentration during sampling was ~20 ppm).

Methane emitted from tree stem surface was collected from a tree stem chamber that was isolated from the atmosphere using a neoprene cushions that were attached to the tree stem surface around the tree approximately 30 cm from each other, on top of which a plastic membrane was stretched with steel wires (Haikarainen, 2016). Tree stem chamber was installed to a height of 1 m above the ground to a silver birch (*Betula pendula*) that had earlier been shown to emit high amounts of methane to the atmosphere. Similarly to soil chambers, a fan was installed inside tree stem chamber to enhance the mixing of air and the tree stem chamber was first flushed from the atmospheric methane by circulating the gas between the chamber and the portable methane sampling system so that most of the atmospheric methane inside the chamber were removed. After contaminating methane had been removed, the valves for inlet and outlet tubes of the methane sampling system were closed and methane concentrations inside the chamber were left to build up. After one hour the methane concentrations inside the chamber had increased to ~10 ppm and a sample was

collected. Because of the much smaller volume of the tree stem chamber compared to the soil chamber, methane concentrations inside the chamber decreased rapidly during the sampling and approached 0 ppm after 10 minutes of collection. For this reason the build-up sampling process was repeated total of 10 times until a sufficient sample size had been achieved (the concentrations were left to build up for longer times during nights).

Atmospheric air samples were collected at one go, next to the tree stem chamber. The sampling was carried out for 12 hours at flow rate of 0.75 l/ minutes with atmospheric methane concentrations of ~2 ppm which equals a calculated carbon sample of well over the threshold of 0.5 mg used at Laboratory of Chronology.

3.4.1 Conditions at field during methane sampling

The samples were collected during three different time periods of 5.-7.6.2018 at Hyytiälä and Siikaneva, 24.-28-9.2018 at Hyytiälä and Siikaneva and 15.-16.01.2019 at Kumpula. As discussed in chapter 1.1.4 methane fluxes from different environmental sources are sensitive to changes in daily weather including soil surface water content and temperature, air temperature and amount of uv-radiation as well as to further climatological changes such as changes in temperature and in precipitation patterns. Air temperature at 2 meter height at Hyytiälä, as well as the soil surface temperature at Siikaneva during the campaigns are plotted in figures 10 and 11. UV radiation is not expected to have a strong impact in these measurements as the peatland soil samples were collected from a dark chamber that does not penetrate radiation and in trees UV-radiation mainly affects the abiotic methane productions in leaves. Soil surface water content and methane fluxes at Siikaneva are plotted in figures 13 and 14. The figures show an increased methane fluxes during the summer time even though soil surface water content remained similar. Temperature at Kumpula during the collection of the last atmospheric sample are plotted in figure 12, but there is no other data as the sample was collected in mid-winter and from higher ground so $^{14}C/^{13}C$ should have a little to no effect from nearby environmental sources. All data is derived from open research data portal (AVAA).

The temperatures were uncharacteristically low during the June campaign as the temperatures decreased to approximately 2 °C during night time and only rose to little over 10 °C during day time, Variation of soil temperatures were smaller and remained below 9 °C during the whole time. Thermic summer began early in 2018 (6.5.2018) and conditions preceding both measurement campaigns were dry as a result of low total precipitation during the 2018 summer period (Finnish Meteorological Institute).

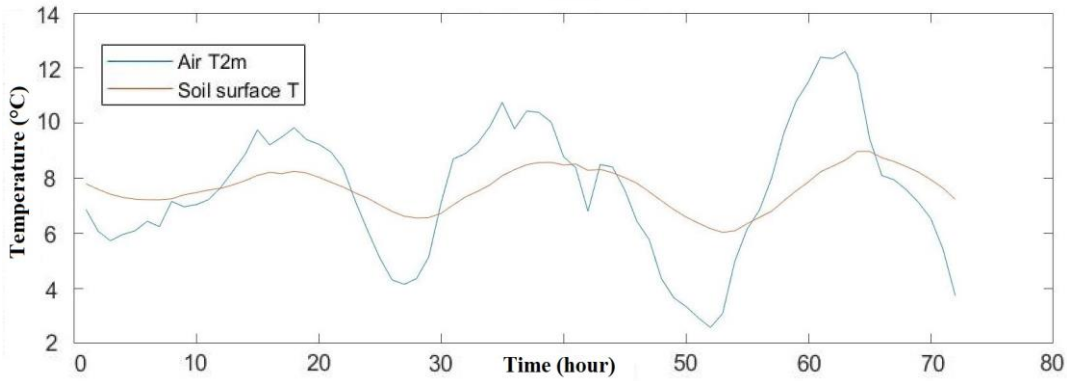

Figure 10: Soil surface temperature at Siikaneva and air temperature from 2 m height at Hyytiälä during the first measurements, 5.-7.6.2018.

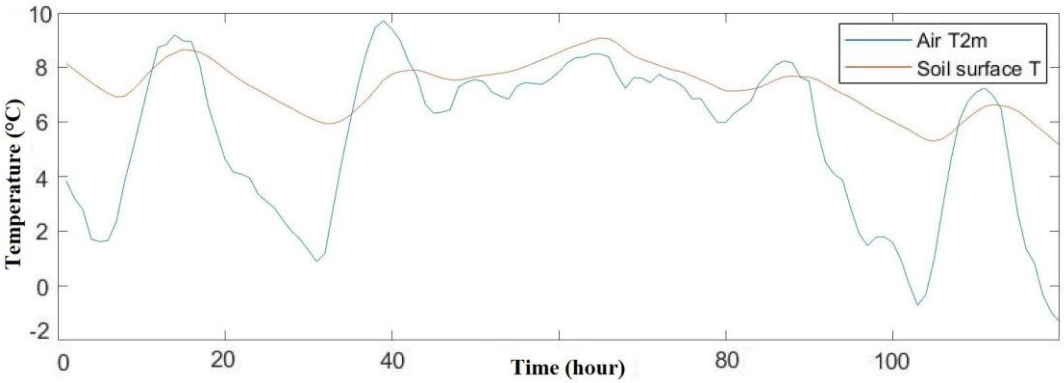

Figure 11: Soil surface temperature at Siikaneva and air temperature from 2 m height at Hyytiälä during the second measurements, 24.-28.9.2018.

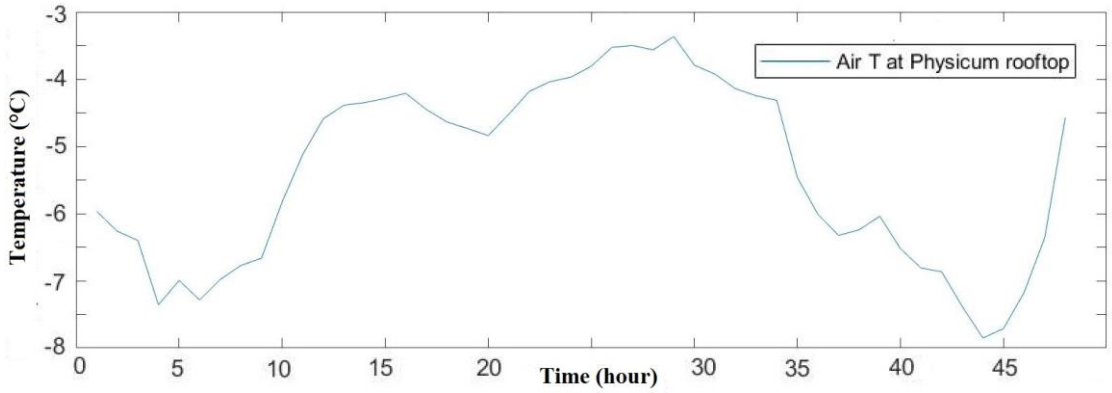

Figure 12: Temperature at Phycicum rooftop, Kumpula, Helsinki, during the measurements at 15.-16.1.2019.

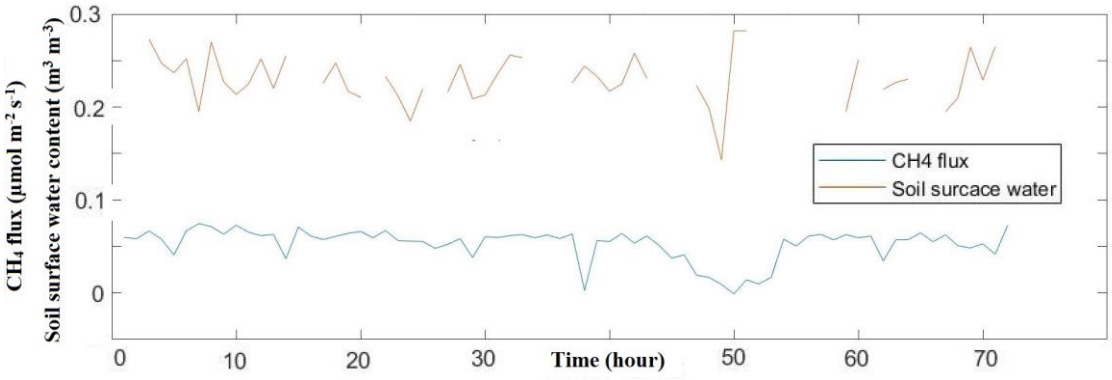

Figure 13: Methane flux from the Siikaneva peatland measured by eddy covariance method.and soil surface water content at Siikaneva during the first measurements 5.-7.6.2018.

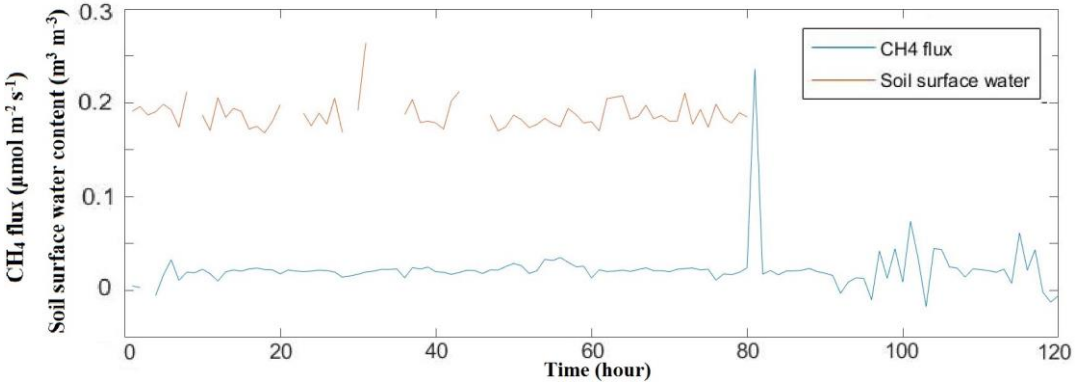

Figure 14: Methane flux from the Siikaneva peatland measured by eddy covariance method.and soil surface water content at Siikaneva during the second measurements 24.-28.9.2018. The data for soil surface water content during the last two days was not available.

4. Results and Discussion

In this chapter the results for individual tests for carbon monoxide and carbon dioxide removal, methane combustion and finally AMS measurements described in previous chapter are presented and analyzed.

4.1 Laboratory measurements

4.1.1 Carbon monoxide removal

The effectivity of carbon monoxide oxidation using Moleculite ® catalyst are represented in figure 15.

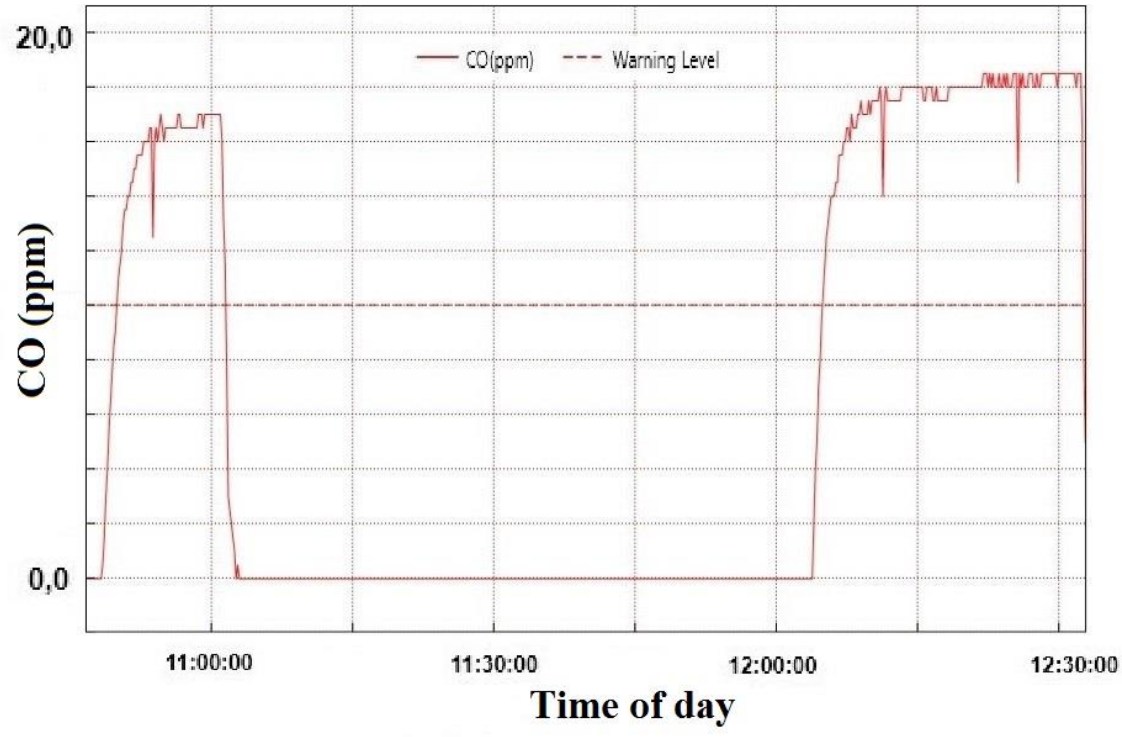

Figure 15: Carbon monoxide removal/ oxidation efficiency with Moleculite ® catalyst. Solid line represents the carbon monoxide in the outlet flow after the ~20 ppm carbon monoxide gas has passed the Moleculite ® catalyst. Dashed line is the 10 level, which was set as a warning level during the test by CO datalogger. Test started at 11:00 and ended at 12:00.

From the test it is obvious that Moleculite ® trap is a very efficient way to oxidize carbon monoxide to carbon dioxide as the carbon monoxide concentrations in the outlet flow dropped to 0.0 sharply after the flow was directed through the catalyst. During the test, flow rates were increased step-by-step in 15 minutes intervals from 0.25 liters per minutes to 0.5 to 1.0 and finally to 2.0 liters per minutes. The flow rate had no effect on the carbon monoxide oxidation effectivity of Moleculite ® catalyst. After 12:00 carbon monoxide concentrations quickly jumped back to the original value as the catalyst was bypassed. The manufacturers reported accuracy of EL-USB-CO carbon monoxide datalogger was 0.5 ppm, meaning the carbon monoxide concentrations after Moleculite ® catalyst was inserted to the gas stream was less than 0.5 ppm and more than 95% of the carbon monoxide was oxidized to carbon dioxide. As the carbon monoxide concentrations in environmental sources are usually much smaller than methane concentration, the use of Moleculite ® catalyst provides a very efficient mean to decrease the contamination from carbon monoxide to negligible levels in methane radiocarbon measurements.

4.1.2 Carbon dioxide removal

The carbon dioxide removal was tested with three different setups using atmospheric air of ~400 ppm carbon dioxide with roughly 1 ppt water and a flow velocity of 1.0 l/min. The adsorption efficiency was examined first by monitoring carbon dioxide concentrations in the gas flow with the Li-840A analyzer. The result for each setup are shown in figure 16.

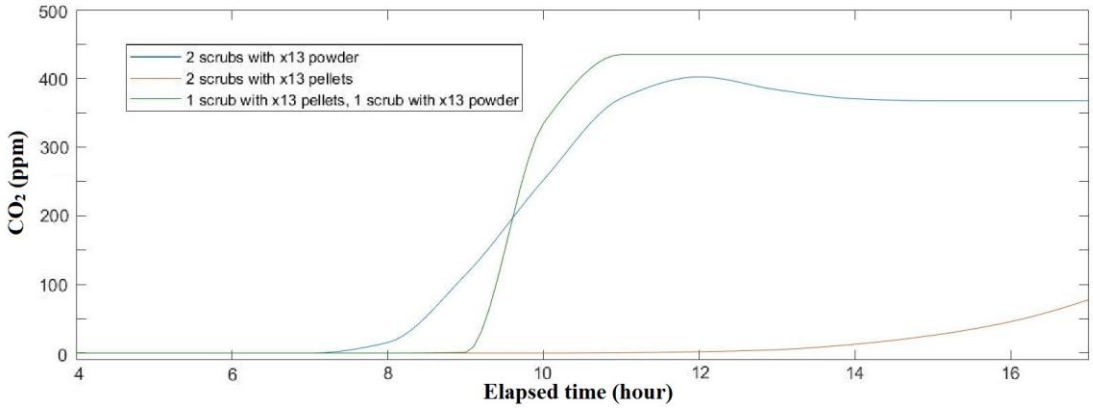

Figure 16: Carbon dioxide removal with 13X zeolite scrubs measured with Li-840A analyzer. The red line: two scrubs with 20 grams 13X zeolite pellets; the blue line: two scrubs with 20 grams 13X zeolite powder; the green line: one scrub with 13X zeolite powder and one with pellets.

From the figure 16 it can be seen that:

a) Two scrubs with 20 g of 13x zeolite pellets (0.5 mm mesh size) in a row (red line, Figure 18): After opening the molecular sieve scrub valves the carbon dioxide concentrations in the flow dropped rapidly to zero as the scrubs started to adsorb carbon dioxide. Carbon dioxide concentrations stayed constant for 12 hours after which a slow increase in carbon dioxide level began indicating an imperfect adsorption by the molecular sieve grains.

b) Two scrubs with 20 g 13x zeolite powder (45-60 mesh-size) in a row (blue line, Figure 18): Again carbon dioxide concentrations in the flow rapidly dropped to zero as the flow was directed through the sieve tubes. This time carbon dioxide content stayed constant only for 7 hours and after which a considerably faster increase in carbon dioxide concentrations commenced compared to previous setup.

c) A scrub with x13 zeolite pellets & a scrub with 13x zeolite powder in a row (green line, Figure 18): Now the carbon dioxide concentrations stayed at zero for 9 hours after which a rapid rise in carbon dioxide levels was detected.

These tests clearly indicated that the 13x zeolite powder became saturated faster than the pellets. The saturation point was reached when the carbon dioxide concentrations started to increase.

Secondly, to make sure that the carbon dioxide removal was indeed complete, a sample molecular sieve tube was inserted after the Li-840A analyzer to measure the amount of carbon dioxide in the gas flow that is below the detection level of the Li-840A analyzer. For each carbon dioxide removal test, a sample was collected from the first three hours of the adsorption tests and the amount of carbon that had not been captured by the carbon dioxide removal setup was measured using the HASE-preparation line.

The average amount of carbon derived from blank, regenerated, molecular sieves measured in the HASE-preparation line was on average 5 µg pure carbon. In the test, the carbon dioxide that could be released from molecular sample sieves were less than 6 µg, when at least one scrub was filled with x13 zeolite powder. This indicates that all of the carbon dioxide is removed when one of the carbon dioxide removal scrubs is filled with x13 zeolite powder as long as the scrubs are not saturated. When both of the scrubs where filled with x13 zeolite pellets, the measured amount of carbon captured by molecular sieve was 30 µg. This contributes a contamination up to 10 µg per hour for atmospheric samples at a flow rate of 1.0 liters per minutes. For atmospheric methane concentrations of 2 ppm, the same amount of air would contribute a methane sample of ~60 µg. Clearly using this kind of setup for carbon dioxide removal is not sufficient.

The overall best results for carbon dioxide removal is therefore achieved with a one scrub filled with x13 zeolite pellets and the other with x13 zeolite powder, preferably in this order as the scrub filled with x13 zeolite powder will then capture all of the carbon dioxide in the flow until saturation point is reached. With this setup all of the carbon dioxide is removed for nine hours of sampling of air (400 ppm carbon dioxide, 1000 ppm water) with a flow rate of 1.0 liters per minutes, a total of 900 liters. This is enough for a sufficient methane sample (~0.5 mg of pure carbon) for radiocarbon measurements from atmospheric air. As mentioned previously, carbon monoxide concentrations inside target chambers can reach much higher levels. In these

circumstances it is important to acknowledge that the molecular sieve scrubs will reach the saturation point earlier and if necessary switch new, regenerated scrubs during the sampling.

The adsorption capacity of the molecular sieves were also tested for the small molecular sieve cartridges containing 1 g of molecular sieve material with a water removal unit or a cooling mechanism placed after the combustion unit to see if the reduced adsorption capacity could be enhanced. Both, the water removal and cooling mechanism had no observable effect.

4.1.3 Combustion of methane

The results for measured impact to methane combustion efficiency due to changes in combustion pressure or methane concentration are presented in figure 19. In the left graph of figure 17, the combustion efficiency with two different methane concentrations are presented as a functions of combustion temperature. In the right side graph of the figure 19 the combustion efficiency is presented with two different combustion pressures with concentrations kept constant at 5000 ppm.

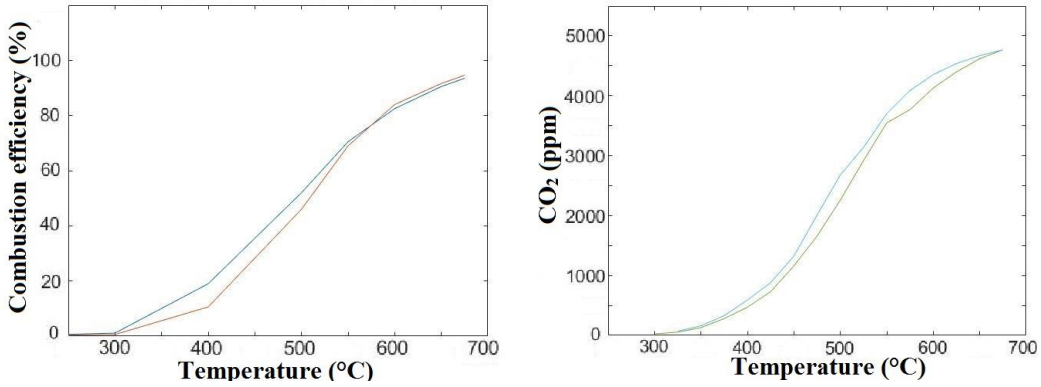

Figure 17: Combustion efficiency for the catalyst (20 mg of Pd/Al_2O_3 powder) as a function of oven temperature (measured carbon dioxide/ methane concentration in the sample gas) with a flow rate of 1 liters per minute. On left side graph, the red line is the combustion efficiency with a methane concentration of 5 000 ppm; the blue line is the efficiencies for 1000 ppm. On the right side graph, the blue line is the combustion efficiencies for 90 kPa pressure; the black line for 60 kPa.

In all tests a moderate methane combustion started occurring approximately when temperatures inside the combustion unit reached 300 °C. After 400 °C was reached, the combustion efficiency started to increase more rapidly. At 500 °C, the combustion efficiency was around 60% in all tests. After that the rate which the combustion efficiency increased with increasing temperatures started to decrease. The plots for 1000 ppm methane and 5000 ppm methane on left side graph of figure 19 are highly similar indicating that concentration does not significantly affect the methane combustion efficiency in the system. The same can be seen from the right side graph of figure 19. The combustion efficiencies for 60 kPa (kilo-Pascal) and 90 kPa cases are nearly identical. The system is usually used at pressures slightly below ambient pressure so that a pressure step for Nafion-dry water removal is created (Palonen et al., 2015).

These results supported the notion from Palonen et al., 2017, that the combustion efficiency is mainly dependent on the flow rates and combustion temperatures that are used to collect the sample. The results presented by Palonen et al., (2017) for combustion efficiency as a function of oven temperature and flow rate are shown in figure 20. The results show that methane combustion is complete for flow rates of 0.10 and 0.25 already around 500 °C temperatures. With 0.50 liters per minutes flow the combustion efficiency approaches 100% at 600 °C, but with a flow rate of 1.0 liters per minutes a complete combustions is not achieved without increasing the temperature way over 600 °C, which has been observed to cause a damage to the catalyst. It should be noted that these measurement from Palonen et al. 2017, where all done with the same catalyst that was used for pressure and concentration measurements as well. After the catalyst had been replaced with a new one, a significantly better combustion has been measured, with 100% efficiency with a flow rate as high as 0.75 liters per minutes with oven oven temperature of 600 °C.

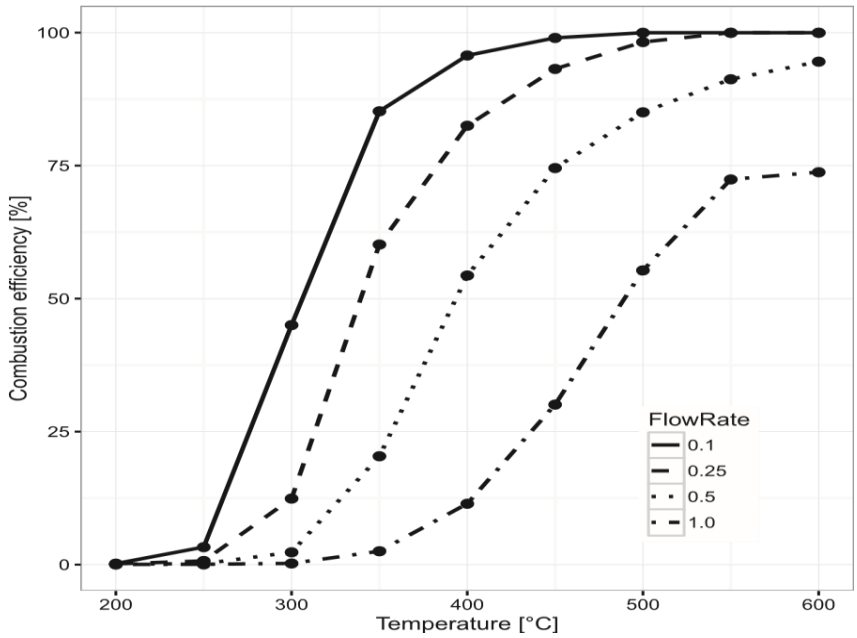

Figure 18: Combustion efficiency for the currently used catalyst (20 mg of Pd/Al_2O_3 powder) as a function of oven temperature and flow rate. Flow rates given in l/min.

4.1.4 AMS concentration measurements series using fossil methane

Figure 19 presents the sampling time for a 1 mg of carbon given as a function of average methane concentration and flow rate of 1.0 l/min. The sampling time is calculated from the equation 5 shown in chapter 2.3. As noted before, usually a threshold of 0.5 mg of carbon has been used in graphitization of the samples and AMS analyzes at Laboratory of Chronology, and that a flow rate of less than 1.0 liters per minutes is used at present to make sure a complete combustion of methane. Incomplete combustion can lead to fractionation as the lighter carbon isotopes of methane are more readily combusted to carbon dioxide. A correction for fractionation is always done with AMS measurements though (Palonen et al., 2017).

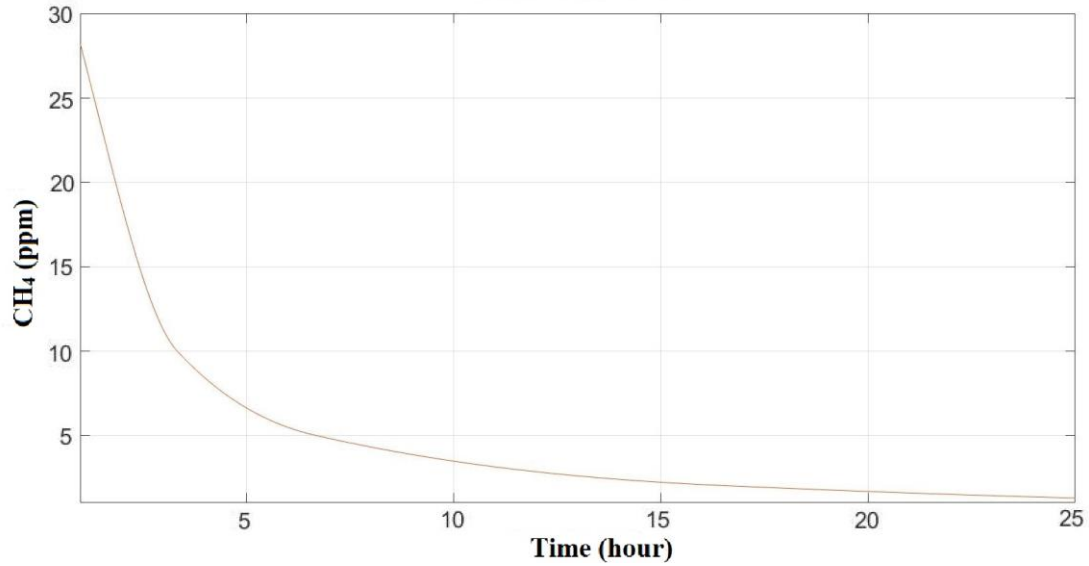

Figure 19: Sampling time for methane as a function of time and concentration using a flow rate of 1 liter per minute.

The results from the AMS measurements of fossil methane can be seen from Table 1. For the first series, the age of the 100 ppm methane sample was 51 569 years with ^{14}C content of 0.16 ± 0.10 pMC (percent modern carbon). As expected this resembles a "fossil" sample as there is practically no ^{14}C left due to decay. This demonstrates the capability of the sampling system to measure correct ^{14}C contents of methane samples and is coherent with the measurements of the biogas/natural gas mixtures by Palonen et al. (2017).

With the sample from 25 ppm methane the measured age of carbon was 38446 years with a ^{14}C content of 0.86 ± 0.11 pMC, which is still quite resembling of a "fossil" sample, but a small background from newer carbon could be seen. This most likely results from the carbon dioxide handling and graphitization process as the amount of carbon in the sample was 0.15 mg, which is four times smaller than the amounts usually used for AMS measurements. This is well-known behavior of ^{14}C sample preparation lines: smaller samples are more prone to inevitable residual gas contamination within the vacuum lines (e.g. Donahue et al., 1990). Systematically higher background for the measurements is evident in the measurements using a larger molecular sieves with carbon age of methane variating from 10579 years with 25 ppm concentration to 7483 years with a concentration of 2 ppm. In figure 20 linear

interpolation is used for the results for both AMS measurements series to determine how the background of the method changes as a function of methane concentrations. The much higher background is most likely due to imperfect regeneration process for the larger molecular sieve scrubs. This is supported by the field measurement that will be discussed next. The means for how to avoid the contamination from earlier measurements are discussed in the chapter 5.

Table 1: Corrected ages of carbon in methane samples for samples with different concentrations of fossil methane.

SAMPLE	MASS	AGE	pMC [100*FM]	±
Fos.CH_4, 100ppm, small sieve tube	0.6	51569	0.16	0.10
Fos.CH_4, 25ppm, small sieve tube	0.2	38446	0.83	0.11
Fos.CH_4, 25ppm, large sieve tube	0.4	10579	26.80	0.15
Fos.CH_4, 8ppm, large sieve tube	0.1	8269	35.72	0.23
Fos.CH_4, 2ppm, large sieve tube	0.2	7483	39.39	0.25

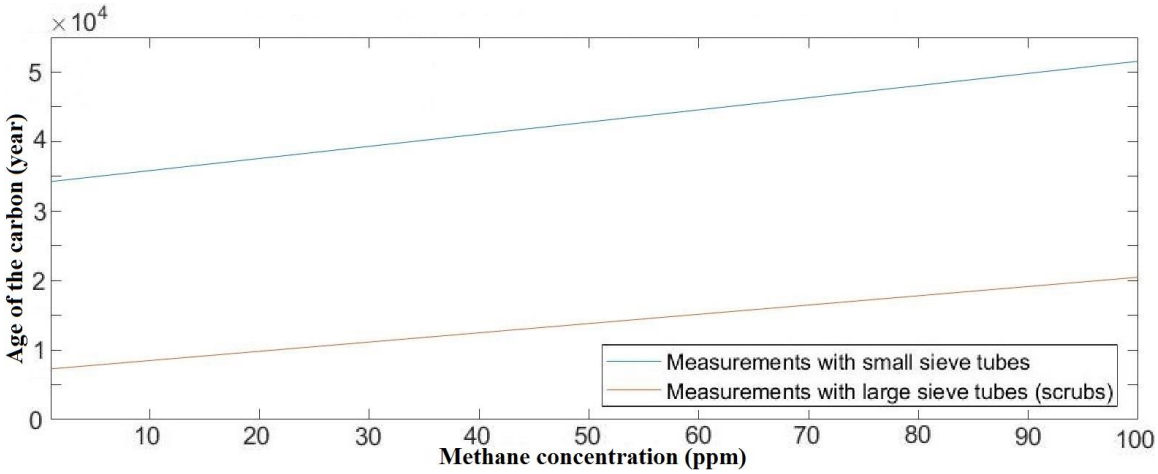

Figure 20: Linear interpolation of methane ages as a function of concentration for two different measurement series, using different molecular sieves. The age of the methane was determined from the $^{14}C/^{13}C$ isotopic fractions.

4.2 Atmospheric radiocarbon of methane

A total of three samples for radiomethane content from atmospheric air were collected and measured with AMS using the portable methane sampling system. Due to the same

issues that were detected during the laboratory measurements series due to small sample sizes, at first, 2 grams of molecular sieve material was added to the smaller molecular sieve cartridges to collect larger samples from atmospheric methane. The first two samples were collected at one go from Hyytiälä between 27.-28.9.2018. The first sample was collected between hours 09:00 and 22:00 resembling radiocarbon content of methane during day time and the second was collected between 22:00 and 12:00 resembling conditions during night and early day. The same problems existed even with the additional molecular sieve material in cartridges and both samples were too small to measure with traditional graphitization procedure, so instead of graphitization the samples were measured directly from the carbon dioxide released from the sieves using gas-ion source technique (Vuoriheimo, 2017). Third sample was collected from the rooftop of Physicum, Helsinki between 15.-16.1.2019 at two separate days. The sample was collected to a larger molecular sieve as in the second measurement series to collect a sample large enough for graphitization.

The first and second samples from Hyytiälä were 102.27 ± 0.02 pMC and 101.40 ± 0.02 pMC respectively. Both results were resembling of ^{14}C contents of atmospheric carbon dioxide and much lower than expected values from what the interpolated values from Lassey et al., 2007 would suggest, which would be over 140 pMC. The results for the third measurement of atmospheric radiomethane content that was collected from the rooftop of Physicum, Helsinki, was significantly lower than even the ones measured from Hyytiälä. The ^{14}C content was 52.40 ± 0.21 pMC. This indicates a significant fossil source of methane. This is most likely due to imperfect regeneration of the molecular sieve cartridge, as the same molecular sieve had previously been used for the methane concentrations series and therefore had captured fossil carbon that was not released during the graphitization process and the regeneration of the sieve cartridge. Table 2 shows the ^{14}C contents of each measurement, as pMC.

Table 2: Corrected ^{14}C content in methane samples collected from atmospheric air.

SAMPLE	MASS	pMC [100*FM]	±
Hyytiälä, 27.9.2018 (day)	0.03	102.27	0.02
Hyytiälä, 28.9.2018 (night)	0.1	101.40	0.02
Kumpula, 15.-16.1.2019	0.5	52.40	0.21

4.3 Soil surface emitted methane from Siikaneva peatland

A total of three samples of peatland surface emitted methane was collected and measured for ^{14}C content with AMS using the portable methane sampling system. The samples were collected using a chamber that was isolated from the atmosphere by a collar and surrounding water. The methane concentrations inside the chambers were left to build-up so that the sample could be collected at one go. As discussed in chapter 3.2, during the June campaign temperatures were uncharacteristically low, following a very dry time period earlier in May, which affected negatively to the emissions from both surface emitted methane flux at Siikaneva and tree-stem surface emitted methane flux in Hyytiälä. At the start of the sample collection at Siikaneva, during the June campaign, the methane concentrations inside the chamber was approximately 25 ppm. The collections of the sample was carried over one hour and the methane concentration inside the chamber decreased slowly to 15 ppm. The temperature during the second campaign was again cold, nearing 0 °C during night time, which limited the amount of methane emitted from the soil surface. The methane concentration inside the chamber increased only to approximately 5 ppm during one day build-up period and therefore the collection time was increased to 5 hours.

The results for the three measurements can be seen from table 3. The first sample from June had a ^{14}C content of 108.71 ± 0.37 pMC and the September measurements yielded results of 91.84 ± 0.03 and 104.26 ± 0.03 pMC respectively. For the two samples with ^{14}C contents over 100 pMC, results indicated that most of the methane emitted from the soil surface had an origin of recently fixed methane. The result of 91.84 pMC indicated that a higher proportion of emitted methane was originating from deeper parts of the peat as only atmospheric carbon dioxide that has been isolated from the carbon cycle since the bomb peak has a ^{14}C content below 100 pMC (Wuebbles & Hayhoe, 2002). This variation of ^{14}C content between night and day time methane emissions maybe due to increased activity near the soil surface as temperatures rose during the day. This would also indicate that a greater proportion of methane emitted from the surface during night time is originated from deeper soil depths and

transported to the surface by diffusion. The results from earlier ^{14}C studies from of peatland surface emitted methane have varied largely between very old ~3000 year old carbon (~69 pMC) and recently fixed methane (~100 pMC) indicating a large temporal and patial variation in ^{14}C content in emitted methane from peatland surfaces (Garnett et al., 2012, Leith et al., 2014).

Table 3: Corrected ^{14}C contents from peatland surface emitted methane samples.

SAMPLE	MASS	pMC [100*FM]	±
Siikaneva 5.6.2018	0.20	108.71	0.37
Siikaneva 25.9.2018 (morning)	0.02	91.84	0.03
Siikaneva 26.9.2018 (evening)	0.03	104.26	0.03

4.4 Tree stem emitted methane from Hyytiälä

In addition to samples collected from atmospheric air and soil surface emitted methane from peatland surface, one sample was collected from tree stem emitted methane. A silver birch from which a particularly high methane fluxes were measured in earlier studies (Haikarainen, 2016) was selected as the conditions for tree emitted methane due to dry and cold weather were not overly favorable. The sample was collected between 5.-7.6.2018 in 10 goes as the concentrations of methane in the small volume tree-stem chamber decreased rapidly during the collection of the samples. The methane concentrations inside the chamber at the start of each collection interval varied from 60 ppm to 5 ppm depending on the build-up duration and time of the day (uv-radiation, temperature etc.). The plan was to collect another sample from tree emitted methane during the September campaign, but due to even colder temperatures during the time of the campaign and because of very dry conditions almost the entire preceding summer fluxes from the tree stem were not sufficient for sampling.

The result for ^{14}C content of tree stem emitted methane during June 5.-7.6.2018 is listed in table 4. The ^{14}C content was 113.60 ± 0.37 pMC. This resembles carbon dioxide of average age of ~20 years as because of the bomb spike ^{14}C content of atmospheric carbon dioxide has been decreasing since the nuclear bomb treaty that took place in 1963 (Levin at al., 2010). Due to the lack of previous published result from ^{14}C content of tree emitted methane there is no comparable measurements.

Compared to the sample collected from Siikaneva during the same time our result indicates that methane emitted from tree stem surface had an older origin. This would imply a significant source of methane that has been taken from deeper depths of soil by the roots compared to peatland emitted methane and been contributing to the age of soil emitted methane from Siikaneva, which would then decrease the ^{14}C levels of released methane as suggested by the results in chapter 4.4.

Table 4: Corrected ^{14}C content from tree-stem surface emitted methane.

SAMPLE	MASS	pMC [100*FM]	±
Hyytiälä, 5.-7.6.2018	0.2	113.60	0.37

5. Concluding remarks

The purpose of this work was to determine the functionality of our system in collecting and measuring samples for radiocarbon content of methane from environmental sources by first testing the system in laboratory conditions and then by collecting and measuring samples from different environmental sources. Individual components of the system were each tested to validate their functionality independently and after this the system as a whole was tested in laboratory measurements and in field. According to the measurements, each component functioned as was expected. The first measurements from both, in field and in laboratory using methane concentrations demonstrative of concentrations at field conditions revealed that the size of the samples collected were significantly less than what was expected. In theory this could have been due to either imperfect combustion process or due to problems with adsorption of the combusted methane. Possible reasons for problems with adsorption of the sample could rise from increased temperature of carbon dioxide and water vapor that are generated in the combustion process, or due to the capability of molecular sieve material to adsorb slight amounts of nitrogen (Deng et al., 2012).

In addition to laboratory measurement, during the sampling process, both the carbon dioxide removal and combustion process could be monitored using the Li-840A analyzer. Both, laboratory measurements and field test indicated that our setup for

removing water vapor, carbon monoxide and carbon dioxide is functional and that the combustion of methane is efficient as long as the flow velocity and combustion temperature is adjusted correctly. The adsorption capacity of the molecular sieves were also tested with a cooling mechanism placed after the combustion unit to see if the reduced adsorption capacity was related to heating of the sample gas. The cooling mechanism had no effect, indicating that adsorbed nitrogen(N_2) was the main cause for reduced adsorption of carbon dioxide. Due to the fact that removing nitrogen from the sample gas flow would be challenging as approximately 79% of atmosphere consist of nitrogen, an additional test was made for the small and large molecular sieves to see how long the collections of sample is efficient by placing the sieves in front of the Li-840A and observing the carbon dioxide levels as methane was combusted to carbon dioxide and collected to the sieves. For the small sieve it was evident that adsorption of the methane converted to carbon dioxide decreased after approximately 20 minutes regardless of the concentration when concentrations were less than 400 ppm. With larger molecular sieve with a maximum amount of molecular sieve material (~30 g), the sieves were able to adsorb combusted methane for well over 12 hours indicating that the adsorption of nitrogen is not a problem and a sufficient sample collection efficiency for atmospheric samples can be achieved.

The first results from laboratory measurement series with different concentrations of fossil methane were encouraging, indicating that the ^{14}C background is negligible as the ^{14}C content was 0.16 pMC with methane concentrations of 100 ppm and when the sample size was sufficient with more than 0.5 mg of carbon. The background values increased with lower concentrations most likely due to decreased sample sizes. Second measurements with larger molecular sieves had a much stronger background of modern carbon. This high background could also be seen to other direction from the atmospheric methane sample collected from Kumpula, Helsinki, Finland, as the results showed a clear fossil signal originating from earlier measurements using the fossil methane. This result clearly indicated that the problem originates from incomplete regeneration of the sieve tubes, which should be plausible to overcome in the future either by making changes to sieve tube design or by changes to the regeneration oven unit. It is crucial that all of the molecular sieve material is heated to sufficient temperature, otherwise the adsorbed sample is either not released properly from the

base of the sieve where most of the sample is captured, or the sample is recaptured in the outlet part of the sieve. Logical next step would then be to install a longer regeneration oven to the HASE-line and decreasing slightly the amount of molecular sieve material inside the larger sieve cartridge. Increasing the regeneration time and/or temperatures should also be considered.

In addition to laboratory measurements, field samples from environmental sources using chamber method where collected from peatland soil surface and tree-stem surface emitted methane. Collections were made during two different campaigns to Hyytiälä SMEAR II station, Juupajoki, Finland. Atmospheric samples were also collected during the second campaign from Hyytiälä. The result from atmospheric measurements indicated a much lower ^{14}C contents compared to previous atmospheric measurements reported by Lassey et al., 2007. This may indicate a large spatial and temporal variation in ^{14}C content of atmospheric methane or may have risen from problems due to small sample sizes. In either way, more measurements to determine the temporal and spatial variation of atmospheric radiomethane content should be made as it would give new insight to the importance of individual methane sources and processes on local scales, and also help up-scaling individual source contribution to global scale (Wuebbles & Hayhoe, 2002). For the same reason the ^{14}C content of individual sources needs to be quantified. For this work three samples from peatland emitted methane and one sample from tree-emitted methane were collected during the June and September campaigns. Due to small samples received from both peatland emitted and tree-stem emitted methane, and due to lack of reference measurements, especially from tree-emitted methane, it is impossible to make strong conclusions from the results. More measurement are required in the future and a campaign to collect methane emitted from peatland soil surface during the whole growing period will be made during the summer of 2019 in Sodankylä, Finland as a collaboration with FMI. From the result received during the campaigns of June and September 2018, the difference between peatland and tree-stem emitted methane indicated an older source of methane emitted from tree-stems. Though as discussed in chapter 4, the lower ^{14}C content measured from peatland soil could also be explained by a significant source of old methane originating from deeper soil depths. This would subsidize with a possible diurnal variation detected from peatland emitted methane in samples collected in

September. A low ^{14}C content of 91.84 pMC in methane was measured from sample collected during night time compared to the 101.40 pMC collected after daytime, indicating that a higher proportions of methane emitted during night time is originating from deeper soil depths due to diffusion. If accurate, the result of 91.84 pMC also demonstrates that a significant portion of methane emitted during night time from peatland soil surface is of an origin of methane that has been isolated from carbon cycle for long periods as ^{14}C content below 100 pMC indicates a carbon consumed before the bomb spike of late 1950's and start of the 1960's (Levin et al., 2010). The results also indicate that during day time, when the methane flux is also larger, the increase is probably mainly due to processes that occur closer to the peatland soil surface.

Overall the results from the measurements were encouraging even though some changes are clearly needed. Currently the system is the first reported that can be used for collecting environmental radiocarbon samples from both atmosphere and from various low concentration sources with chamber methods. Collection of both the carbon dioxide and water created in combustion process offers in theory a plausible way to also measure the δ^2H values from methane, but this has not been tested yet. An additional benefit is that the system also allows carbon dioxide sample collection when the combustion unit is by-passed. Future work still includes the changes to molecular sieves and/or changes to regeneration unit to improve the regeneration process. Batteries with longer battery life should be considered for samples collected from sources where external power sources are not available.

The biggest challenge for radiocarbon measurements of methane from environmental sources will be collecting an extensive reference measurement data, so that further analyzes of individual measurements will be plausible. This should lead to better understanding of methane formation and emission pathways from various sources, which would lead to better estimations of individual source terms in global methane budget and enhance the future estimations.

References

”AVAA”, AVAA open data publishing platform for research data < https://avaa.tdata.fi/web/smart/smear/download > Reference day 29.4.2019.

Barba, J., Bradford, M. A., Brewer, P. E., Bruhn, D., Covey, K., Van Haren, J., et al. (2019). Methane emissions from tree stems: A new frontier in the global carbon cycle. New Phytologist, 222(1), 18-28.

Bartle, K. D., & Myers, P. (2002). History of gas chromatography. TrAC Trends in Analytical Chemistry, 21(9-10), 547-557.

Bayer, J., Williams, P., & Druffel, E. (1992). Recovery of submilligram quantities of carbon dioxide from gas streams by molecular sieve for subsequent determination of isotopic (^{13}C and ^{14}C) natural abundances. Analytical Chemistry, 64(7), 824-827.

Bruhn, D., Møller, I. M., Mikkelsen, T. N., & Ambus, P. (2012). Terrestrial plant methane production and emission. Physiologia Plantarum, 144(3), 201-209.

Burch, R., & Loader, P. (1994). Investigation of Pt/Al2O3 and Pd/Al2O3 catalysts for the combustion of methane at low concentrations. Applied Catalysis B: Environmental, 5(1-2), 149-164.

Carmichael, M., Bernhardt, E., Bräuer, S., & Smith, W. (2014). The role of vegetation in methane flux to the atmosphere: Should vegetation be included as a distinct category in the global methane budget? Biogeochemistry, 119(1-3), 1-24.

Covey, K. R., Wood, S. A., Warren, R. J., Lee, X., & Bradford, M. A. (2012). Elevated methane concentrations in trees of an upland forest. Geophysical Research Letters, 39(15).

Deng, H., Yi, H., Tang, X., Yu, Q., Ning, P., & Yang, L. (2012). Adsorption equilibrium for sulfur dioxide, nitric oxide, carbon dioxide, nitrogen on 13X and 5A zeolites. Chemical Engineering Journal, 188, 77-85.

Donahue, D. J., Linick, T. W., & Jull, A. T. (1990). Isotope-ratio and background corrections for accelerator mass spectrometry radiocarbon measurements. Radiocarbon, 32(2), 135-142.

Ehhalt, D. (1974). The atmospheric cycle of methane. Tellus, 26(1-2), 58-70.

Ehhalt, D., & Schmidt, U. (1978). Sources and sinks of atmospheric methane. Pure and Applied Geophysics, 116(2-3), 452-464.

Etminan, M., Myhre, G., Highwood, E., & Shine, K. (2016). Radiative forcing of carbon dioxide, methane, and nitrous oxide: A significant revision of the methane radiative forcing. Geophysical Research Letters, 43(24).

Federer, U., Kaufmann, P. R., Hutterli, M. A., Buiron, D., Blunier, T., Fischer, H., et al. (2009). A new method for high-resolution methane measurements on polar ice cores using continuous flow analysis. Environmental Science & Technology, 43(14), 5371-5376.

"Finnish Meteorological Institute", Finnish Meteorological Institutes statistics from summer 2018 < http:// ilmatieteenlaitos.fi/kesatilastot>, Reference day 9.4.2019.

Forster, P., Ramaswamy, V., Artaxo, P., Berntsen, T., Betts, R., Fahey, D. W., et al. (2007). Changes in atmospheric constituents and in radiative forcing. Chapter 2. Climate change 2007. The physical science basis.

Fraser, W. T., Blei, E., Fry, S. C., Newman, M. F., Reay, D. S., Smith, K. A., et al. (2015). Emission of methane, carbon monoxide, carbon dioxide and short-chain hydrocarbons from vegetation foliage under ultraviolet irradiation. Plant, Cell & Environment, 38(5), 980-989.

Garnet, K. N., Megonigal, J. P., Litchfield, C., & Taylor Jr, G. E. (2005). Physiological control of leaf methane emission from wetland plants. Aquatic Botany, 81(2), 141-155.

Garnett, M., Hardie, S., & Murray, C. (2012). Radiocarbon analysis of methane emitted from the surface of a raised peat bog. Soil Biology and Biochemistry, 50, 158-163.

Garnett, M., & Murray, C. (2013). Processing of CO_2 samples collected using zeolite molecular sieve for ^{14}C analysis at the NERC radiocarbon facility (East Kilbride, UK). Radiocarbon, 55(2), 410-415.

Gauss, M., Myhre, G., Isaksen, I., Grewe, V., Pitari, G., Wild, O., et al. (2006). Radiative forcing since preindustrial times due to ozone change in the troposphere and the lower stratosphere. Atmospheric Chemistry and Physics, 6(3), 575-599.

Graedel, T., & McRae, J. (1980). On the possible increase of the atmospheric methane and carbon monoxide concentrations during the last decade. Geophysical Research Letters, 7(11), 977-979.

Haikarainen, I. (2016). Boreaaliset puut metaanin lähteenä kasvukauden alussa, MSc thesis, http://urn.fi/URN:NBN:fi:hulib-201606092270.

Hansen, J., Sato, M., Ruedy, R., Nazarenko, L., & Lacis, A. (44). Coauthors, 2005: Efficacy of climate forcings. J. Geophys.Res, 110, D18104.

Hardie, S., Garnett, M., Fallick, A., Rowland, A., & Ostle, N. (2005). Carbon dioxide capture using a zeolite molecular sieve sampling system for isotopic studies (^{13}C and ^{14}C) of respiration. Radiocarbon, 47(3), 441-451.

IPCC, 2014: Climate Change 2014: Synthesis Report. Contribution of Working Groups I, II and III to the Fifth Assessment Report of the Intergovernmental Panel on Climate Change [Core Writing Team, R.K. Pachauri and L.A. Meyer (eds.)]. IPCC, Geneva, Switzerland, 151 pp.

Keppler, F., Hamilton, J. T., Braß, M., & Röckmann, T. (2006). Methane emissions from terrestrial plants under aerobic conditions. Nature, 439(7073), 187.

Kirschke, S., Bousquet, P., Ciais, P., Saunois, M., Canadell, J., Dlugokencky, E., et al. (2013). Three Decades of Global Methane Sources and Sinks, Nat.Geosci., 6, 813–823.

Lassey, K. R., Lowe, D. C., Brenninkmeijer, C. A., & Gomez, A. J. (1993). Atmospheric methane and its carbon isotopes in the southern hemisphere: Their time series and an instructive model. Chemosphere, 26(1-4), 95-109.

Lassey, K., Etheridge, D., Lowe, D., Smith, A., & Ferretti, D. (2007). Centennial evolution of the atmospheric methane budget: What do the carbon isotopes tell us? Atmospheric Chemistry and Physics, 7(8), 2119-2139.

Lassey, K., Lowe, D., & Smith, A. (2007). The atmospheric cycling of radiomethane and the" fossil fraction" of the methane source. Atmospheric Chemistry and Physics, 7(8), 2141-2149.

Lee, J. H., & Trimm, D. L. (1995). Catalytic combustion of methane. Fuel Processing Technology, 42(2-3), 339-359.

Leith, F. I., Garnett, M. H., Dinsmore, K. J., Billett, M., & Heal, K. V. (2014). Source and age of dissolved and gaseous carbon in a peatland–riparian–stream continuum: A dual isotope (^{14}C and $\delta^{13}C$) analysis. Biogeochemistry, 119(1-3), 415-433.

Levin, I., Naegler, T., Kromer, B., Diehl, M., Francey, R., Gomez-Pelaez, A., et al. (2010). Observations and modelling of the global distribution and long-term trend of atmospheric $^{14}CO_2$. Tellus B: Chemical and Physical Meteorology, 62(1), 26-46.

Lingenfelter, R. E. (1963). Production of carbon 14 by cosmic-ray neutrons. Reviews of Geophysics, 1(1), 35-55.

Liu, J., Chen, H., Zhu, Q., Shen, Y., Wang, X., Wang, M., et al. (2015). A novel pathway of direct methane production and emission by eukaryotes including plants, animals and fungi: An overview. Atmospheric Environment, 115, 26-35.

Lowe, D. C., Brenninkmeijer, C. A., Tyler, S. C., & Dlugkencky, E. J. (1991). Determination of the isotopic composition of atmospheric methane and its application in the antarctic. Journal of Geophysical Research: Atmospheres, 96(D8), 15455-15467.

Machacova, K., Bäck, J., Vanhatalo, A., Halmeenmäki, E., Kolari, P., Mammarella, I., et al. (2016). Pinus sylvestris as a missing source of nitrous oxide and methane in boreal forest. Scientific Reports, 6, 23410.

Maier, M., Machacova, K., Lang, F., Svobodova, K., & Urban, O. (2018). Combining soil and tree-stem flux measurements and soil gas profiles to understand CH_4 pathways in Fagus sylvatica forests. Journal of Plant Nutrition and Soil Science, 181(1), 31-35.

Manning, M., Lowe, D., Melhuish, W., Sparks, R., Wallace, G., Brenninkmeijer, C., et al. (1990). The use of radiocarbon measurements in atmospheric studies 1. Radiocarbon, 32(1), 37-58.

Matson, P. A., & Harriss, R. C. (2009). Biogenic trace gases: Measuring emissions from soil and water. John Wiley & Sons. 291-321.

Nisbet, R., Fisher, R., Nimmo, R., Bendall, D., Crill, P., Gallego-Sala, A. V., et al. (2009). Emission of methane from plants. Proceedings of the Royal Society B: Biological Sciences, 276(1660), 1347-1354.

Oinonen, M., Palonen, V., Uusitalo, J. Biofraction measurements of methane for environmental and metrological applications. Poster presented at 22nd International Radiocarbon Conference in Dakar, Senegal, 16–20 November 2015.

Pack, M. A., Xu, X., Lupascu, M., Kessler, J. D., & Czimczik, C. I. (2015). A rapid method for preparing low volume CH_4 and CO_2 gas samples for ^{14}C AMS analysis. Organic Geochemistry, 78, 89-98.

Palonen, V., & Oinonen, M. (2013). Molecular sieves in $^{14}CO_2$ sampling and handling. Radiocarbon, 55(2), 416-420.

Palonen, V., Pesonen, A., Herranen, T., Tikkanen, P., & Oinonen, M. (2013). HASE–The Helsinki adaptive sample preparation line. Nuclear Instruments and Methods in Physics Research Section B: Beam Interactions with Materials and Atoms, 294, 182-184.

Palonen, V. (2015). A portable molecular-sieve-based CO_2 sampling system for radiocarbon measurements. Review of Scientific Instruments, 86(12), 125101.

Palonen, V., & Tikkanen, P. (2015). A novel upgrade to Helsinki AMS: Fast switching of isotopes with electrostatic deflectors. Nuclear Instruments and Methods in Physics Research Section B: Beam Interactions with Materials and Atoms, 361, 263-266.

Palonen, V., Uusitalo, J., Seppälä, E., & Oinonen, M. (2017). A portable methane sampling system for radiocarbon-based bioportion measurements and environmental CH_4 sourcing studies. Review of Scientific Instruments, 88(7), 075102.

Palonen, V., Pumpanen, J., Kulmala, L., Levin, I., Heinonsalo, J., & Vesala, T. (2018). Seasonal and diurnal variations in atmospheric and soil air $^{14}CO_2$ in a boreal scots pine forest. Radiocarbon, 60(1), 283-297.

Pangala, S. R., Hornibrook, E. R., Gowing, D. J., & Gauci, V. (2015). The contribution of trees to ecosystem methane emissions in a temperate forested wetland. Global Change Biology, 21(7), 2642-2654.

Pangala, S. R., Enrich-Prast, A., Basso, L. S., Peixoto, R. B., Bastviken, D., Hornibrook, E. R., et al. (2017). Large emissions from floodplain trees close the amazon methane budget. Nature, 552(7684), 230.

Petrenko, V. V., Smith, A. M., Brailsford, G., Riedel, K., Hua, Q., Lowe, D., et al. (2008). A new method for analyzing ^{14}C of methane in ancient air extracted from glacial ice. Radiocarbon, 50(1), 53–73.

Pumpanen, J., Kolari, P., Ilvesniemi, H., Minkkinen, K., Vesala, T., Niinistö, S., et al. (2004). Comparison of different chamber techniques for measuring soil CO_2 efflux. Agricultural and Forest Meteorology, 123(3-4), 159-176.

Quay, P., King, S., Stutsman, J., Wilbur, D., Steele, L., Fung, I., et al. (1991). Carbon isotopic composition of atmospheric CH_4: Fossil and biomass burning source strengths. Global Biogeochemical Cycles, 5(1), 25-47.

Quay, P., Stutsman, J., Wilbur, D., Snover, A., Dlugokencky, E., & Brown, T. (1999). The isotopic composition of atmospheric methane. Global Biogeochemical Cycles, 13(2), 445-461.

Ramanathan, V. (1988). The greenhouse theory of climate change: A test by an inadvertent global experiment. Science, 240(4850), 293-299.

Reeburgh, W. S. (2003). Global methane biogeochemistry. Treatise on Geochemistry, 4, 347.

Rice, A. L., Butenhoff, C. L., Shearer, M. J., Teama, D., Rosenstiel, T. N., & Khalil, M. A. K. (2010). Emissions of anaerobically produced methane by trees. Geophysical Research Letters, 37(3).

Rusch, H., & Rennenberg, H. (1998). Black alder (Alnus glutinosa (L.) Gaertn.) trees mediate methane and nitrous oxide emission from the soil to the atmosphere. Plant and Soil, 201(1), 1-7.

Saunois, M., Bousquet, P., Poulter, B., Peregon, A., Ciais, P., Canadell, J. G., et al. (2016). The global methane budget 2000–2012. Earth System Science Data (Online), 8(2).

Schwartz, S. E. (2018). Resource letter GECC-1: The greenhouse effect and climate change: Earth's natural greenhouse effect. American Journal of Physics, 86(8), 565-576.

Shindell, D. T., Faluvegi, G., Koch, D. M., Schmidt, G. A., Unger, N., & Bauer, S. E. (2009). Improved attribution of climate forcing to emissions. Science (New York, N.Y.), 326(5953), 716-718.

Skeie, R., Berntsen, T., Myhre, G., Tanaka, K., Kvalevåg, M., & Hoyle, C. (2011). Anthropogenic radiative forcing time series from pre-industrial times until 2010. Atmospheric Chemistry and Physics, 11(22), 11827-11857.

Slota, P., Jull, A. T., Linick, T., & Toolin, L. (1987). Preparation of small samples for ^{14}C accelerator targets by catalytic reduction of CO. Radiocarbon, 29(2), 303-306.

Stenström, K. E., Skog, G., Georgiadou, E., Genberg, J., & Johansson, A. (2011). A guide to radiocarbon units and calculations. Lund University, Department of Physics Internal Report, 1-17.

Stevenson, D., Young, P., Naik, V., Lamarque, J., Shindell, D. T., Voulgarakis, A., et al. (2013). Tropospheric ozone changes, radiative forcing and attribution to emissions in the atmospheric chemistry and climate model intercomparison project (ACCMIP). Atmospheric Chemistry and Physics, 13(6), 3063-3085.

Terazawa, K., Yamada, K., Ohno, Y., Sakata, T., & Ishizuka, S. (2015). Spatial and temporal variability in methane emissions from tree stems of Fraxinus mandshurica in a cool-temperate floodplain forest. Biogeochemistry, 123(3), 349-362.

Tikkanen, P., Palonen, V., Jungner, H., & Keinonen, J. (2004). AMS facility at the University of Helsinki. Nuclear Instruments and Methods in Physics Research Section B: Beam Interactions with Materials and Atoms, 223, 35-39.

Townsend-Small, A., Tyler, S. C., Pataki, D. E., Xu, X., & Christensen, L. E. (2012). Isotopic measurements of atmospheric methane in Los Angeles, California, USA: Influence of "fugitive" fossil fuel emissions. Journal of Geophysical Research: Atmospheres, 117(D7).

Vuoriheimo, T. (2017). ^{14}C-CO_2 measurements with accelerator mass spectrometry, MSc thesis, http://urn.fi/URN:NBN:fi-fe2017112252130.

Wahlen, M., Tanaka, N., Henry, R., Deck, B., Zeglen, J., Vogel, J. S., et al. (1989). Carbon-14 in methane sources and in atmospheric methane: The contribution from fossil carbon. Science (New York, N.Y.), 245(4915), 286-290.

Wang, Z., Gu, Q., Deng, F., Huang, J., Megonigal, J. P., Yu, Q., et al. (2016). Methane emissions from the trunks of living trees on upland soils. New Phytologist, 211(2), 429-439.

Wuebbles, D. J., & Hayhoe, K. (2002). Atmospheric methane and global change. Earth-Science Reviews, 57(3-4), 177-210.